PHYSICAL REVIEW D **87,** 054025 (2013)

Glueballs and the Yang-Mills plasma in a *T*-matrix approach

Gwendolyn Lacroix,[1,*] Claude Semay,[1,†] Daniel Cabrera,[2,‡] and Fabien Buisseret[1,§]

[1]*Service de Physique Nucléaire et Subnucléaire, Université de Mons, UMONS Research Institute for Complex Systems, Place du Parc 20, 7000 Mons, Belgium*

[2]*Departamento de Física Teórica II, Universidad Complutense, 28040 Madrid, Spain*

(Received 19 October 2012; published 20 March 2013)

The strongly coupled phase of Yang-Mills plasma with arbitrary gauge group is studied in a T matrix approach. The existence of lowest-lying glueballs, interpreted as bound states of two transverse gluons (quasiparticles in a many-body setup), is analyzed in a nonperturbative scattering formalism with the input of lattice-QCD static potentials. Glueballs are actually found to be bound up to 1.3 T_c. Starting from the T-matrix, the plasma equation of state is computed by resorting to a formulation of statistical mechanics (Dashen *et al.*) and favorably compared to quenched lattice data. Special emphasis is put on SU(N) gauge groups, for which analytical results can be obtained in the large-N limit, and predictions for a G_2 gauge group are also given in this work.

DOI: 10.1103/PhysRevD.87.054025 PACS numbers: 12.38.Mh, 12.39.Mk, 11.15.Pg

I. INTRODUCTION

More than two decades after pioneering works [1,2], the phenomenology related to the deconfined phase of QCD, i.e., the quark-gluon plasma (QGP), is still a fascinating topic both experimentally and theoretically. On the experimental side, the QCD matter was or is studied in heavy-ion collisions (RHIC, SPS, FAIR, LHC). These experiments seem to show that the QGP behaves like a perfect fluid. On the theoretical side, the study of QCD at finite temperature deserves much interest because it is a challenging problem in itself and because of the many connections with experiments.

The aim of this work is to study the thermodynamic features of QGP by resorting to a T-matrix approach. The power of this approach is that the bound states and scattering states of the system can be studied in a whole picture. Such an approach has already been proven to give relevant results in the study of hadronic matter above the critical temperature of deconfinement (T_c) [3] but has not yet been applied to compute the equation of state (EoS). This observable will be computed here thanks to the Dashen *et al.* formulation of statistical mechanics in terms of the S matrix (or T matrix) [4]. Such a formulation is particularly well suited for systems whose microscopic constituents behave according to relativistic quantum mechanics. The QGP is indeed identified with a quantum gas of gluons and quarks, which are seen as the effective degrees of freedom propagating in the plasma. This assumption is actually common to all the so-called quasiparticle approaches [5,6], with the crucial difference being that the use of a T-matrix formulation allows us to investigate the behavior of the QGP in a temperature range, where it is strongly interacting. This strong interaction means here that bound states are still expected to survive above T_c.

Too strong an interaction could cause such large width for the quasiparticles that the concept of the quasiparticle itself could become questionable. A consensus seems to exist about the relevance of this notion for plasma above 3 T_c, but the situation is less clear below [7]. A first encouraging remark is that the notion of quasiparticles has been successful in condensed matter physics, where strongly correlated systems are well described by effective field theories. This does not prove that the situation is similar in hot QCD, but this kind of approach has already produced very good results [8]. It has also been suggested that the assumed smooth crossover between confinement and deconfinement may make it possible to approximate the QCD thermodynamics near crossover in terms of the quasiparticles of quarks and gluons [9]. In order to perform a coherent description of the quark-gluon plasma, it is possible to compute the width of the quasiparticles with a self-consistent procedure [10,11]. This more sophisticated task can be bypassed by the use of a constant width to estimate the effect of a quasiparticle self-energy [12,13].

Although the above formulation can be applied to the full QGP, this paper is dedicated to the description of the gluon plasma. Dealing with only one particle species drastically simplifies the problem, while the main feature of the description, i.e., the explicit inclusion of interactions in a quasiparticle approach, is kept. Moreover, the pure gauge thermodynamic features (in particular, the EoS) are well known in lattice QCD. This will allow an accurate comparison between our phenomenological approach and the lattice QCD calculations. In this paper, the effective thermal mass of the quasigluon is directly

*gwendolyn.lacroix@umons.ac.be
†claude.semay@umons.ac.be
‡Daniel.Cabrera@fis.ucm.es
§Present address: Haute École Louvain en Hainaut (HELHa), Chaussée de Binche 159, 7000 Mons, Belgium.
fabien.buisseret@umons.ac.be

extracted from the lattice data, but this procedure cannot give any information about the gluon width. As explained in Sec. III B 2, we shall use a simple prescription for the computation of the propagator and leave a self-consistent description of the gluon self-energy for a future work.

A particularity of this paper is the generalization of the formalism to any gauge groups, with particular attention to SU(N) and the large-N limit, and to G_2. This group originally attracted attention because, the center of G_2 being trivial, models relating deconfinement to the breaking of a center of symmetry are no longer valid, as for SU(N). However, it still exhibits a first-order phase transition as SU(N) does [14]. Hence, G_2 appears quite attractive from a theoretical point of view.

The paper is organized as follows. Section II is dedicated to the presentation of the general quasiparticle approach based on the T-matrix formalism proposed in Ref. [4]. In Sec. III, the model is particularized to a Yang-Mills plasma with the inclusion of two-body interactions. In Sec. IV, useful analytic comments concerning the thermodynamic observables in the SU(N) and G_2 cases are discussed. The model parameters are fixed in Sec. V, and the existence of the bound states inside the gluon plasma is discussed in Sec. VI. In Sec. VII, the computation of the EoS is presented. Finally, Sec. VIII is devoted to the conclusions and perspectives.

II. T-MATRIX FORMALISM

A. Generalities

The results of Dashen *et al.* [4] can be summarized as follows: The grand potential Ω, expressed as an energy density, of an interacting particle gas is given by (in units where $\hbar = c = k_B = 1$),

$$\Omega = \Omega_0 + \sum_\nu \Bigg[\Omega_\nu - \frac{e^{\beta\vec{\mu}\cdot\vec{N}}}{2\pi^2\beta^2} \times \int_{M_\nu}^{\infty} \frac{d\epsilon}{4\pi i} \epsilon^2 K_2(\beta\epsilon)\, \mathrm{Tr}_\nu(\mathcal{S}S^{-1}\overleftrightarrow{\partial}_\epsilon S)|_c \Bigg]. \quad (1)$$

In the above equation, the first term, Ω_0, is the grand potential of the free relativistic particles, i.e., the remaining part of the grand potential if the interactions are turned off. The second term accounts for interactions in the plasma and is a sum running on all the species, the number of particles included, and the quantum numbers necessary to fix a channel. The characteristics of all these channels are generically denoted ν. The vectors $\vec{\mu} = (\mu_1, \mu_2, \ldots)$ and $\vec{N} = (N_1, N_2, \ldots)$ contain the chemical potentials and the particle number of each species taking part in a given scattering channel.

Despite the fact that the T-matrix formalism allows a unified treatment of bound and scattering states, we will follow precisely the procedure of Dashen *et al.* [4] and consider separately the contributions above and below the threshold[1] M_ν. Below the threshold, one has Ω_ν, the grand potential coming from bound states, seen as free additional species in the plasma and appearing as poles of the S matrix. Above the threshold, one has the scattering contribution, where the trace is taken in the center of mass frame of the channel ν and where S is the S matrix, depending in particular on the total energy ϵ. The symmetrizer $\mathcal{S}$ enforces the Pauli principle when a channel involving identical particles is considered, and the subscript c means that only the connected scattering diagrams are taken into account. Notice that $K_2(x)$ is the modified Bessel function of the second kind, that β is linked to the temperature T thanks to $\beta = 1/T$, and that the notation $A\overleftrightarrow{\partial}_x B = A(\partial_x B) - (\partial_x A)B$ is used.

By definition, $S = 1 - 2\pi i\delta(\epsilon - H_0)\mathcal{T}$, where $\mathcal{T}$ is the off-shell T matrix and where H_0 is the free Hamiltonian of the system. A convenient way to compute $\mathcal{T}$ is to solve the Lippmann-Schwinger equation for the off-shell T matrix, schematically given by

$$\mathcal{T} = V + VG_0\mathcal{T}, \quad (2)$$

with G_0 the free propagator and V the interaction potential.

Once the T matrix is known, two problems can be simultaneously addressed: the existence of bound states in the plasma and its EoS. The T-matrix formalism has the advantage of treating bound and scattering states on the same footing and is particularly suited for the present situation, where we expect bound states to become less and less bound when the temperature increases, eventually crossing over and melting into the continuum. This dissociation mechanism has been shown to provide considerable threshold enhancement effects in heavy quark-antiquark correlation functions [3].

The plasma EoS is obtained from (1), then the pressure is simply given by [15,16]

$$p = -\Omega, \quad (3)$$

and the other thermodynamic observables can be derived from p, like the entropy density or the trace anomaly ($\Delta = e - 3p$, where e is the energy density) [5,16]. For later convenience, the thermodynamic quantities will be normalized to the Stefan-Boltzmann pressure, which is defined as

$$p_{\mathrm{SB}} = -\lim_{m_i \to 0} \Omega_0, \quad (4)$$

m_i being the masses of the particles propagating in the medium.

B. Interaction potential

The explicit computation of Ω obviously requires the knowledge of the on-shell T matrix that can be derived in

[1]Within this approach, the threshold is the summation on the mass of all the particles included in a given channel ν.

particular from (2). A key ingredient of the present approach is thus the potential V, encoding the interactions between the particles in the plasma. In the following, V is chosen as pairwise: for an n-body channel, $V = \sum_{i<j} V_{ij}$ with V_{ij} the potential between two particle species i and j. Having in mind the building of an effective framework describing the deconfined phase of a non-Abelian gauge theory, each particle composing the plasma should be in a given representation of the considered gauge (or color) group. It is therefore reasonable to assume that the potential V between two particles in the representations R_i and R_j of the considered gauge group has the color dependence of a (screened) one-gluon-exchange potential, that is, in momentum space,

$$V_{ij} = \tilde{M}_{R_i} \cdot \tilde{M}_{R_j} \alpha_S \bar{v}(\beta, \vec{q}, \vec{q}'), \tag{5}$$

where $\tilde{M}_R$ denotes the generator of the considered gauge algebra in the representation R, and where the real function $\bar{v}$ only depends on the temperature and two momenta (no dependence on the mass or other attributes of the particle). We keep the name gluon for the gauge particle even if the gauge group can formally be arbitrary. In the above definition, it has to be remembered that $\alpha_S = g^2/4\pi$ and that $g^2 = \lambda/C_2^{\text{adj}}$, with adj the adjoint representation of the gauge group under study and C_2^R the value of the quadratic Casimir in the representation R. Note that in the case of SU(N), λ is the 't Hooft coupling (fixed in the large-N limit).

Introducing quadratic Casimirs, one can rewrite (5) as

$$V_{ij} = \frac{C_2^{\mathcal{C}} - C_2^{R_i} - C_2^{R_j}}{2} \alpha_S \bar{v} \equiv \kappa_{\mathcal{C};ij} v, \tag{6}$$

with $\mathcal{C}$ the pair representation and

$$\kappa_{\mathcal{C};ij} = \frac{C_2^{\mathcal{C}} - C_2^{R_i} - C_2^{R_j}}{2C_2^{\text{adj}}}. \tag{7}$$

Again, the real function $v = v(\beta, \vec{q}, \vec{q}')$ only depends on the temperature and on two momenta—an explicit form for v will be given later. The validity of the form (6) for V_{ij} has partially been checked in pure gauge SU(3) lattice calculations, showing that the static potential between two sources, in different representations and bound in a color singlet, follows the Casimir scaling expected from a process of the one-gluon-exchange type [17]. The peculiar scaling (6) also leads to a relevant large-N behavior of the EoS when the gauge group SU(N) is chosen, as it will be shown in Sec. IV.

Among the various possible representations, the case where a singlet (denoted $\bullet$) appears in the tensor product $R_i \otimes R_j$ is particularly relevant. Since $C_2^{\bullet} = 0$ and the other quadratic Casimirs are positive, the singlet is the most attractive channel in any two-body scattering process and thus the most favorable one for the formation of bound states. Such two-particle bound states should presumably be the lowest-lying ones and, being color-singlet, should give rise to low-lying glueballs or mesons for instance.

C. Born approximation

The scattering term in (1), given by

$$\Omega_s = -\sum_{\nu} \frac{e^{\beta\vec{\mu}\cdot\vec{N}}}{2\pi^2\beta^2} \int_{M_\nu}^{\infty} \frac{d\epsilon}{4\pi i} \epsilon^2 K_2(\beta\epsilon) \mathrm{Tr}_\nu (\mathcal{S}S^{-1} \overleftrightarrow{\partial}_\epsilon S)|_c, \tag{8}$$

can be considerably simplified by using the Born approximation, i.e., by noticing that if the interactions are weak enough, $\mathcal{T} = V + \mathrm{O}(V^2)$. Such conditions are generally expected to be valid at high enough temperatures, where the typical interaction energy is small with respect to the typical thermal energy of the particles. Note also that, in some cases, this approximation can be relevant when the factor $\kappa_{\mathcal{C};ij}$ is negligible, irrespective of the temperature. Such cases will be encountered when the gauge group is SU(N) (see Sec. IV).

To the first order in V, (8) becomes

$$\Omega_s = \sum_{\nu} \frac{e^{\beta\vec{\mu}\cdot\vec{N}}}{2\pi^2\beta^2} \int_{M_\nu}^{\infty} d\epsilon \epsilon^2 K_2(\beta\epsilon)\, \mathrm{Tr}_\nu \partial_\epsilon (\delta(\epsilon - H_0)V)|_c + \mathrm{O}(V^2). \tag{9}$$

Let us write explicitly $\nu = (n, \tilde{\nu})$, where n is the total number of particles involved in a given scattering channel, and where $\tilde{\nu}$ are the remaining quantum numbers. A useful remark to be made at this stage is that the pairwise structure of V causes $V|_c$ to be always vanishing except in two-body channels. Here, at the Born approximation, n is always equal to 2. Then, $\mathrm{Tr}_\nu \partial_\epsilon (\delta(\epsilon - H_0)V)|_c = \mathrm{Tr}_{\tilde{\nu}} \kappa_{\mathcal{C},ij} \partial_\epsilon (\delta v)$, with $\delta = \delta(\epsilon - \epsilon_{ij}(q))$ and $\epsilon_{ij}(q) = \sqrt{q^2 + m_i^2} + \sqrt{q^2 + m_j^2}$. Note that the color channel $\mathcal{C}$ and the particle species i, j are part of $\tilde{\nu}$. After having extracted from the trace the color and J^{PC} dependences (J^P if the charge conjugation is not relevant), one is led to

$$\Omega_s = \sum_{(i,j)} \frac{e^{\beta(\mu_i+\mu_j)}}{2\pi^2\beta^2} \sum_{J^{PC}} (2J+1) \sum_{\mathcal{C}} \dim \mathcal{C} \kappa_{\mathcal{C},ij} \times \int_{M_{\tilde{\nu}}}^{\infty} d\epsilon \epsilon^2 K_2(\beta\epsilon)\, \mathrm{Tr}_q \partial_\epsilon (\delta v_{J^{PC}}) + \mathrm{O}(V^2), \tag{10}$$

where $\dim \mathcal{C}$ is the pair representation dimension, Tr_q the remaining trace on the momentum space, and $v_{J^{PC}}$ the potential with the angular symmetry of the considered channel.

Among the various summations to be performed in $\sum_{\tilde{\nu}}$, two are of particular interest: the one over the different interacting species, that can be denoted $\sum_{(i,j)}$, and the one over the color representations appearing in $R_i \otimes R_j$, that is $\sum_{\mathcal{C}}$. Because of $\kappa_{\mathcal{C},ij}$, (10) is thus proportional to a factor $\sum_{\mathcal{C}} \dim \mathcal{C} \kappa_{\mathcal{C},ij}$ for a given pair i, j in

a given J^{PC} channel. When the combinations of species do not have to respect a symmetry principle, this last sum runs on all the representations appearing in $R_i \otimes R_j$; one can then show that

$$\sum_{\mathcal{C}} \dim \mathcal{C} \kappa_{\mathcal{C},ij} = 0. \tag{11}$$

Indeed, it is known in group theory that the second-order Dynkin indices I^R in a tensor product obey a sum rule that can be rewritten using our notations as $I^{R_i} \dim R_j + I^{R_j} \dim R_i = \sum_{\mathcal{C}} I^{\mathcal{C}}$ [18]. Using $C_2^R = (\dim \mathrm{adj}/\dim R) I^R$ [18], one straightforwardly shows that (11) holds. Note that (10) and (11) are thus *a priori* nonzero when a symmetry principle has to be respected. The summation cannot then be performed on all possible color representations.

III. YANG-MILLS PLASMA

A. Grand canonical potential

Let us now particularize the general formalism presented in the previous section to a genuine Yang-Mills plasma, i.e., with no matter fields. The bosonic degrees of freedom propagating in the plasma are then quasigluons, which are transverse spin-1 bosons in the adjoint representation of the gauge group. The baryonic potential can be set equal to 0, and according to standard formulas in statistical mechanics, one has

$$\Omega_0 = 2 \dim \mathrm{adj} \omega_0(m_g), \tag{12}$$

where the quasigluons are *a priori* supposed to have a mass m_g, and where

$$\omega_0(m) = \frac{1}{2\pi^2 \beta} \int_0^\infty dk k^2 \ln\left(1 - \mathrm{e}^{-\beta\sqrt{k^2+m^2}}\right) \tag{13}$$

is the grand potential per degree of freedom associated to a bosonic species with mass m. Equation (4) leads to

$$p_{\mathrm{SB}} = \frac{\pi^2}{45\beta^4} \dim \mathrm{adj}. \tag{14}$$

Let us recall that in the following, the term "gluon" indifferently denotes the gauge field of Yang-Mills theory and the quasigluon.

The sum $\sum_\nu$ appearing in (1) now explicitly reads $\sum_{n_g} \sum_{\mathcal{C}} \sum_{J^{PC}}$, where n_g is the number of gluons involved in the interaction process. As soon as $n_g > 2$, the determination of the allowed color channels and of the correct symmetrized gluon states generally becomes a painful task, to which the problem of finding the T matrix in many-body scattering must be added. Intuitively, one can nevertheless expect the dominant scattering processes to be two-gluon ones, and thus only consider $n_g = 2$ in a first approach. After simplification, the grand potential (1) eventually reads

$$\begin{aligned}\Omega^{(2)} = {} & 2 \dim \mathrm{adj}\, \omega_0(m_g) + \sum_{\mathcal{C}} \sum_{J^P} \dim \mathcal{C}(2J+1) \\ & \times \left\{ \omega(M_{\mathcal{C},J^P}) + \frac{1}{2\pi^2\beta^2} \int_{2m_g}^\infty d\epsilon \epsilon^2 K_2(\beta\epsilon) \right. \\ & \times \mathrm{Tr}_{\mathcal{C},J^P}[(\delta \mathrm{Re}\mathcal{T})' - 2\pi((\delta \mathrm{Re}\mathcal{T})(\delta \mathrm{Im}\mathcal{T})' \\ & \left. - (\delta \mathrm{Im}\mathcal{T})(\delta \mathrm{Re}\mathcal{T})')] \right\}, \end{aligned} \tag{15}$$

where the symbol "prime" is the derivative respective to the energy and $M_{\mathcal{C},J^P}$ is the mass of the two-gluon bound state with color $\mathcal{C}$ and quantum numbers J^P, if it exists. The index C in the J^{PC} channel is dropped since the charge conjugation is always positive for a two-gluon state [19]. In the remaining trace, it is understood that the T matrix is computed in a given two-body channel with color $\mathcal{C}$ and quantum numbers J^P and that the Dirac δ reads $\delta(\epsilon - 2\epsilon(q))$, with the dispersion relation $\epsilon(q) = \sqrt{q^2 + m_g^2}$. Note also that, in connection with nuclear many-body approaches, (15) can be rewritten in terms of a weighted thermal average of scattering phase shifts by means of unitarity of the S matrix. The computation of the two-gluon T matrix is explained in detail in the following section.

B. Helicity states and the Lippman-Schwinger equation

1. Two gluon states

Jacob and Wick's helicity formalism [20] can be applied to describe a two-gluon state, where the gluons are seen as transverse spin-1 particles. Let us generically define $|\psi(\vec{p}, \lambda)\rangle = a_\lambda^\dagger(\vec{p})|0\rangle$ the quantum state of a particle with momentum $\vec{p}$, spin s, and helicity λ. If the particle is transverse, only $\lambda = \pm s$ is allowed, while all the projections from $-s$ to $+s$ are allowed if the particle has a usual spin degree of freedom. Then it can be deduced from Ref. [20] that the quantum state,

$$\begin{aligned}|J^P, M; \lambda_1, \lambda_2, \epsilon\rangle = {} & \frac{1}{\sqrt{2}}[|J, M; \lambda_1, \lambda_2\rangle \\ & + \epsilon |J, M; -\lambda_1, -\lambda_2\rangle], \end{aligned} \tag{16}$$

with $\epsilon = \pm 1$ and

$$\begin{aligned}|J, M; \lambda_1, \lambda_2\rangle = {} & \left[\frac{2J+1}{4\pi}\right]^{\frac{1}{2}} \int_0^{2\pi} d\phi \int_0^\pi d\theta \sin\theta \\ & \times \mathcal{D}^{J*}_{M,\lambda_1-\lambda_2}(\phi, \theta, -\phi) R(\phi, \theta, -\phi) \\ & \times a_{\lambda_1}^\dagger(\vec{p}) a_{\lambda_2}^\dagger(-\vec{p})|0\rangle, \end{aligned} \tag{17}$$

is a two-particle helicity state in the rest frame of the system, which is also an eigenstate of the total spin $\vec{J}$ and of the parity, i.e., $\vec{J}^2 = J(J+1)$, $J_z = M$, and $P = \epsilon\eta_1\eta_2(-1)^{J-s_1-s_2}$ with η_i and s_i the intrinsic parity and spin of particle i. Moreover, $J \geq |\lambda_1 - \lambda_2|$. In the above definition, $R(\alpha, \beta, \gamma)$ is the rotation operator of Euler angles $\{\alpha, \beta, \gamma\}$, and $\mathcal{D}^J_{M,\lambda}(\alpha, \beta, \gamma)$ are the Wigner D

matrices. The coordinates $\{\theta, \phi\}$ are the polar angles of $\vec{p}$. When both particles have a spin degree of freedom, the helicity basis, spanned by the helicity states (16), is equivalent to a standard $|^{2S+1}L_J\rangle$ basis up to an orthogonal transformation [21]. When at least one of the particles is transverse, both bases are no longer equivalent, but the helicity states can still be expressed as particular linear combinations of $|^{2S+1}L_J\rangle$ states [20]. This will be convenient in view of future computations.

When the two particles are identical ($m_1 = m_2 = m$, $s_1 = s_2 = s$), it is relevant to study the action of the permutation operator P_{12}. One finds [20]

$$[1 + (-1)^{2s}P_{12}]|J^P, M; \lambda_1, \lambda_2, \epsilon\rangle = |J^P, M; \lambda_1, \lambda_2, \epsilon\rangle + (-1)^J|J^P, M; \lambda_2, \lambda_1, \epsilon\rangle, \quad (18)$$

where the operator $[1 + (-1)^{2s}P_{12}] = \mathcal{S}$ is nothing else than a projector on the symmetric (s integer) or antisymmetric (s half-integer) part of the helicity state. It is readily seen in (18) that symmetrizing the state will eventually lead to selection rules for J (this is particularly clear if one sets $\lambda_1 = \lambda_2$). When extra degrees of freedom are added, it is also of interest to use the antisymmetrizer $[1 - (-1)^{2s}P_{12}] = \mathcal{A}$ as done in Table I.

A general discussion about the two-gluon helicity states can be found in Ref. [22], to which we refer the interested reader. For the present work, it is sufficient to recall that four families of helicity states can be found, separated in helicity singlets $|S_\pm; J^P\rangle$ and doublets $|D_\pm; J^P\rangle$ following the pioneering work [23]. The corresponding quantum numbers are given in Table I, as well as the average value of the squared orbital angular momentum, $\langle\vec{L}^2\rangle$, computed with these states.

The average orbital angular momentum is an interesting quantity since it helps to globally understand the mass hierarchy of the glueball spectrum [22]. Moreover, in a naive nonrelativistic picture, it estimates the strength of the orbital barrier in scattering theory. For obvious numerical reasons, all the possible J^P channels contributing to Ω cannot be included, which is why it is of interest to find the channels that will presumably contribute the most, i.e., those with the lowest value of $\langle\vec{L}^2\rangle$. First, one has the symmetric states

TABLE I. Symmetrized and antisymmetrized two-gluon helicity states, following the notation of Refs. [22,23], with the corresponding quantum numbers and averaged squared orbital angular momentum.

State	Symmetrized	Antisymmetrized	$\langle\vec{L}^2\rangle$
$\|S_+; J^P\rangle$	$(\text{even} - J \geq 0)^+$	$(\text{odd} - J \geq 1)^-$	$J(J+1)+2$
$\|S_-; J^P\rangle$	$(\text{even} - J \geq 0)^-$	$(\text{odd} - J \geq 1)^+$	$J(J+1)+2$
$\|D_+; J^P\rangle$	$(\text{even} - J \geq 2)^+$	$(\text{odd} - J \geq 3)^-$	$J(J+1)-2$
$\|D_-; J^P\rangle$	$(\text{odd} - J \geq 3)^+$	$(\text{even} - J \geq 2)^-$	$J(J+1)-2$

$$|S_+; 0^+\rangle = \left[\frac{2}{3}\right]^{1/2}|^1S_0\rangle + \left[\frac{1}{3}\right]^{1/2}|^5D_0\rangle, \quad (19)$$

$$|S_-; 0^-\rangle = -|^3P_0\rangle, \quad (20)$$

expressed in a standard $|^{2S+1}L_J\rangle$ basis, with $\langle\vec{L}^2\rangle = 2$. In the singlet channel, they correspond to the 0^{++} and 0^{-+} glueballs, respectively, which are indeed found to be among the lightest ones at zero temperature, see e.g., the review Ref. [24]. Then, with $\langle\vec{L}^2\rangle = 4$, one has the symmetric state,

$$|D_+; 2^+\rangle = \left[\frac{2}{5}\right]^{1/2}|^5S_2\rangle + \left[\frac{4}{7}\right]^{1/2}|^5D_2\rangle + \left[\frac{1}{35}\right]^{1/2}|^5G_2\rangle, \quad (21)$$

and the antisymmetric states,

$$|S_+; 1^-\rangle = \left[\frac{2}{3}\right]^{1/2}|^1P_1\rangle - \left[\frac{2}{15}\right]^{1/2}|^5P_1\rangle + \left[\frac{1}{5}\right]^{1/2}|^5F_1\rangle, \quad (22)$$

$$|S_-; 1^+\rangle = \left[\frac{1}{3}\right]^{1/2}|^3S_1\rangle - \left[\frac{2}{3}\right]^{1/2}|^3D_1\rangle, \quad (23)$$

$$|D_-; 2^-\rangle = -\left[\frac{4}{5}\right]^{1/2}|^5P_2\rangle - \left[\frac{1}{5}\right]^{1/2}|^5F_2\rangle. \quad (24)$$

The above three states do not exist in the singlet channel, but the symmetric 2^+ state corresponds to the 2^{++} glueball in the singlet channel; the $0^{\pm+}$ and 2^{++} are indeed the lightest states at zero temperature [24]. Only the color-symmetric channels with the lowest value of $\langle\vec{L}^2\rangle$ will be kept in the following study, which aims at being a first step toward a description of the Yang-Mills plasma within a T-matrix formulation.

2. Lippman-Schwinger equation

Solving (2) is a crucial technical part of this work since it eventually leads to the on-shell T matrix. As will be discussed in Sec. V, the potential to be used is known in position space and has first to be Fourier transformed. For a potential with spherical symmetry in configuration space, we use

$$V(q, q', \theta_{q,q'}) = 4\pi\int_0^\infty drrV(r)\frac{\sin(Qr)}{Q}, \quad \text{where} \quad Q = \sqrt{q^2 + q'^2 - 2qq'\cos\theta_{q,q'}} \quad (25)$$

and where $\theta_{q,q'}$ is the angle between the momenta $\vec{q}$ and $\vec{q}'$.

Since two-gluon interactions are considered, the basis states are two-gluon helicity states, given in the above section. As we assume V to be spin independent (see Appendix B), only the orbital angular momentum containing the helicity states has to be taken into account. According to a standard integration, the L-wave part of potential (25) reads

$$V_L(q,q') = 2\pi \int_{-1}^{1} dx P_L(x) V(q,q',x), \tag{26}$$

where P_L is the Legendre polynomial of order L and $x = \cos\theta_{q,q'}$. Our choice is to focus on the scalar, pseudoscalar, and tensor-scattering channels, for which one can compute from (19)–(21) that

$$V_{0^+}(q,q') = \frac{2}{3} V_0(q,q') + \frac{1}{3} V_2(q,q'), \tag{27}$$

$$V_{0^-}(q,q') = V_1(q,q'), \tag{28}$$

$$V_{2^+}(q,q') = \frac{2}{5} V_0(q,q') + \frac{4}{7} V_2(q,q') + \frac{1}{35} V_4(q,q'). \tag{29}$$

Note that once $V_{J^P}(q,q')$, the potential in a given J^P-scattering channel, is known, the off-shell T matrix can be computed from (2) [3],

$$\mathcal{T}(E;q,q') = V_{J^P}(q,q') + \frac{1}{8\pi^3} \times \int_0^\infty dk k^2 V_{J^P}(q,k) G_0(E;k) \mathcal{T}(E;k,q'), \tag{30}$$

where E is the energy in the center of mass frame, and where the two-gluon propagator reads

$$G_0(E;k) = \frac{m_g^2}{\epsilon(k)} \frac{1}{E^2/4 - \epsilon(k)^2 - 2i\epsilon(k)\Sigma_I}, \tag{31}$$

with the gluon dispersion relation $\epsilon(k) = \sqrt{k^2 + m_g^2}$. Note that the normalization conventions of the T matrix are not the same as the ones in Ref. [3] (see Appendix C). The parameter Σ_I accounts for the imaginary part of the gluon self-interaction, whereas the real part is reabsorbed in the effective gluon mass. As mentioned in the Introduction, a more complete calculation of the gluon self-energy would require summing the T matrix over the gluon thermal distribution self-consistently in a Brueckner-Hartree-Fock scheme (schematically, $\Pi_g = \int f^g \mathcal{T} D_g$ with f^g the gluon distribution and D_g the gluon single-particle propagator). We leave such determination for a future work. In the present evaluation, we shall approximate the gluon self-interaction by using an effective in-medium gluon mass (to be discussed in Sec. V) together with a small imaginary part for numerical purposes (we use $\Sigma_I = 0.01$ GeV as in Ref. [3]).

Once $\mathcal{T}(E;q,q')$ is known, the on-shell T matrix is readily obtained as $\mathcal{T}(E;q_E,q_E)$, with $q_E = \sqrt{E^2/4 - m_g^2}$. The Haftel-Tabakin algorithm is used to solve (30) [25]. The momentum integral is discretized within an appropriate quadrature, thus turning the integral equation into a matrix equation, namely, $\sum \mathcal{F}_{ik} \mathcal{T}_{kj} = V_{ij}$, where schematically $\mathcal{F} = 1 - wVG$ (and w denotes the integration weight). The solution follows trivially by matrix inversion. It can be shown that the determinant of the transition function $\mathcal{F}$ (referred to as the Fredholm determinant) vanishes at the bound state energies, which provides a numerical criterion for solving the bound state problem. This strategy has already been successfully used to compute T matrices in the case of quark-antiquark scattering [3].

IV. THERMODYNAMIC OBSERVABLES WITH SU(N) AND G_2

A. Pure gauge sector

1. SU(N) *case*

The explicit computation of $\Omega^{(2)}$, given by (15), obviously requires the knowledge of the on-shell T matrix, which can be derived in particular from (2). In this last equation, G_0 is the propagator of two gluons, which has been discussed in Sec. III. It is only worth saying that $G_0 = \mathrm{O}(1)$ with respect to the number of colors since m_g is assumed to be O(1) (see Sec. VA). The color dependence of the T matrix actually comes from the two-gluon interaction potential only. More precisely, the color dependence of the potential is all included in the factor (7), reading in the present case

$$\kappa_{\mathcal{C};gg} = \frac{C_2^{\mathcal{C}} - 2N}{2N}. \tag{32}$$

The subscript gg is used to recall that two-gluon interactions are concerned in the above formula and $C_2^g = C_2^{\mathrm{adj}} = N$ in the SU(N) case.

The adjoint representation of SU(N), to which gluons belong, can be written as the $(N-1)$-component vector $(1,0,\ldots,0,1)$ in a highest weight representation, corresponding to a Young diagram with one column of length $N-1$ and one column of length 1. More generally, $(a_1,\ldots,a_k,\ldots,a_{N-1})$ corresponds to a Young diagram with a_k columns of length k. The tensor product of the adjoint representation by itself gives the following allowed two-gluon color channels:

$$\begin{aligned}(1,0,\ldots,0,1) \otimes (1,0,\ldots,0,1) = {} & \\ & \bullet^S \oplus (1,0,\ldots,0,1)^A \oplus (2,0,\ldots,0,2)^S && N \geq 2 \\ & \oplus (1,0,\ldots,0,1)^S \oplus (0,1,0,\ldots,0,2)^A \oplus (2,0,\ldots,1,0)^A && N \geq 3 \\ & \oplus (0,1,0,\ldots,0,1,0)^S && N \geq 4. \end{aligned} \tag{33}$$

The superscript S/A denotes a symmetric/antisymmetric channel. The first/second/third line exists as soon as $N \geq 2/3/4$. Note that in the special case $N = 2$, the above tensor product reduces to $(2) \otimes (2) = (0)^S \oplus (2)^A \oplus (4)^S$, and one recovers usual spin-coupling rules. The dimensions and color factors of the representations appearing in (33) can be found in Table IV in Appendix A.

In the singlet channel, one has $\kappa_\bullet = -1$ for any N. It is such that $\mathcal{T} = \mathrm{O}(1)$ since $V = \mathrm{O}(1)$. Consequently, the properties of glueballs in the singlet above the deconfinement temperature are not dependent on N, in agreement with Ref. [26], where it is suggested that this argument is even gauge-group independent. The singlet finally brings a contribution $\mathrm{O}(1)$ to $\Omega^{(2)}$ since its dimension is 1.

Using the same arguments as for the singlet, one finds that the adjoint channels also lead to a T matrix that is N independent. They may lead to bound states since the potential is attractive, though less strongly than for the singlet. The symmetric adjoint channel will presumably be the most favorable for the formation of bound states since it demands a completely symmetric spin-space wave function for the two-gluon state in light of the Pauli principle, and the most attractive J^P channels are indeed symmetric. Note that this symmetric color channel is actually absent for $N = 2$. In the adjoint channel, $\mathcal{T} = \mathrm{O}(1)$ since $V = \mathrm{O}(1)$, but unlike the singlet, its contribution to $\Omega^{(2)}$ is $\mathrm{O}(N^2)$ since $\dim(1, 0, \ldots, 0, 1) = N^2 - 1$.

The two remaining channels with nonzero potential, namely $(2, 0, \ldots, 0, 2)$ [the 27 for SU(3)] and $(0, 1, 0, \ldots, 0, 1, 0)$ (only when $N > 3$), have in common that they are symmetric and that their color factor scales in $1/N$ and thus vanishes in the large-N limit. The fact that $V = \mathrm{O}(1/N)$ in both cases leads to the exact large-N result,

$$\mathcal{T} = V + VG_0V + \mathrm{O}(N^{-3}) \tag{34}$$

or

$$\mathcal{T} = \pm\frac{1}{N}v + \frac{1}{N^2}vG_0v + \mathrm{O}(N^{-3}), \tag{35}$$

the $\pm$ coming from one channel or another. Because of the weakness of V at large N, one can reasonably suppose that even the attractive channel $(0, 1, 0, \ldots, 0, 1, 0)$ does not lead to the formation of bound states. For the two channels under consideration,

$$(\mathcal{S}S^{-1}\overleftrightarrow{\partial}_\epsilon S)|_c \propto \partial_\epsilon \mathrm{Re}\left(\pm\frac{v}{N} + \frac{vG_0v}{N^2}\right) + \mathrm{O}(N^{-3}). \tag{36}$$

One sees in (15) that the contributions of both channels have to be summed, and since they are symmetric, the sums on the allowed J^P are identical in both cases. This causes the term in $1/N$ to vanish in the trace at large-N limit, the first nontrivial one being in $1/N^2$, leading to an overall contribution to $\Omega^{(2)}$ scaling as N^2 because the dimension of both channels scale as N^4.

Although the color singlet is relevant in view of studying glueballs, it does not bring any contribution to the EoS at large N. So, the large-N EoS is dominated by free gluons and scattering processes above threshold in colored channels. The more N is large, the more important is the gap between the confined phase and the deconfined one, whose EoS scales as N^2. It is indeed known that the large-N case corresponds to a strongly first-order phase transition ($N = 3$ is already weakly first order) [27].

2. G_2 case

Another interesting group under consideration is G_2, which is also the best studied gauge group so far beyond $\mathrm{SU}(N)$. The main features of this group are summarized in what follows.

The adjoint representation of G_2 has dimension 14 and reads (0, 1) in a highest weight representation. The two-gluon channels are then given by

$$(0, 1) \otimes (0, 1) = \bullet^S + (0, 1)^A + (0, 2)^S + (2, 0)^S + (3, 0)^A \tag{37}$$

or, in terms of the dimensions, $14 \otimes 14 = 1 + 14 + 77' + 27 + 77$. Using the same normalization as in the $\mathrm{SU}(N)$ case, the color factors, respectively, read [28,29] $\kappa_{C;gg} = -1, -1/2, 1/4, -5/12$, and 0. The color factors in the singlet and adjoint channels are equal to those of $\mathrm{SU}(N)$, so the glueball properties are unchanged in the singlet and antisymmetric adjoint channels. The symmetric $(2, 0)^S$ channel is almost as attractive as the adjoint one and may lead to bound states.

3. Scaling relations for SU(N) and G_2

Some interesting relations about the scaling of the EoS can be deduced thanks to the T matrix. Let us write the on-shell T matrix as $\mathcal{T} = \sum_k a_k \kappa^k_{\mathcal{C};gg,}$ where all a_k do not depend on the color but rather on the other quantum numbers involved. The color dependence of the thermodynamic observables is then given by the quantities $\sum_{\mathcal{C};A/S} \dim \mathcal{C} \kappa^k_{\mathcal{C};gg}$. Using the results of Appendix A and Sec. IV A 2, one can check that for $\mathrm{SU}(N)$ and G_2,

$$\sum_{\mathcal{C};\mathcal{S}} \dim \mathcal{C}_{gg} \kappa_{\mathcal{C};gg} = \frac{1}{2} \dim \mathrm{adj}, \tag{38}$$

$$\sum_{\mathcal{C};\mathcal{S}} \dim \mathcal{C}_{gg} \kappa^2_{\mathcal{C};gg} = \frac{3}{4} \dim \mathrm{adj}, \tag{39}$$

$$\sum_{\mathcal{C};\mathcal{S}} \dim \mathcal{C}_{gg} \kappa^3_{\mathcal{C};gg} = -\frac{1}{8} \dim \mathrm{adj}, \tag{40}$$

$$\sum_{\mathcal{C};\mathcal{A}} \dim \mathcal{C}_{gg} \kappa^k_{\mathcal{C};gg} = \left(-\frac{1}{2}\right)^k \dim \mathrm{adj}. \tag{41}$$

For SU(N) at large N, the previous relations can be written as

$$\sum_{\mathcal{C};\mathcal{S}} \dim \mathcal{C}_{gg} \kappa^k_{\mathcal{C};gg} = N^2\left[\left(-\frac{1}{2}\right)^k + \delta_{k,1} + \frac{1}{2}\delta_{k,2}\right] + \mathrm{O}(1), \tag{42}$$

$$\sum_{\mathcal{C};\mathcal{A}} \dim \mathcal{C}_{gg} \kappa^k_{\mathcal{C};gg} = N^2\left(-\frac{1}{2}\right)^k + \mathrm{O}(1). \tag{43}$$

Again that means that the expected scaling like N^2 (actually like dim adj) of the EoS is found using the present approach. This can be viewed as a confirmation of the relevance of the chosen color scaling (5).

B. Quarks and antiquarks in the 't Hooft limit

Even if the rest of this study will be concerned with a genuine Yang-Mills plasma, it is worth making some comments about the possible inclusion of matter (quarks and antiquarks) in the model. Information about the color channels appearing in interactions involving at least one (anti)quark are given in Tables V and VI; we note that quarks (antiquarks) have been considered to be in the fundamental (conjugate) representation of SU(N), as is the case in the 't Hooft large-N limit [30]. Other interesting large-N limits have been proposed, in which quarks belong to the two-index antisymmetric representation of SU(N), for example Ref. [31], but they will not be studied here.

First of all, the quark-quark and antiquark-antiquark color factors are of order $1/N$. The Born approximation for the T matrix becomes exact at large N (at any temperature) and, since the dimension of any of the corresponding representations scales as N^2, the quark-quark and antiquark-antiquark interactions bring a term scaling as N to the grand potential. More precisely, this term scales as $N_f N$ at the Born approximation once the trace over the different flavors is performed. It is shown in Sec. II C that only the interaction of two identical species can contribute to Ω in this limit. The number of quark flavors remains finite in the 't Hooft limit, which is the case under study here.

The quark-antiquark interactions lead to a T matrix that is O(1) when the pair is in the singlet or $\mathrm{O}(1/N^2)$ when the pair is in the adjoint representation. In both cases, however, the contribution to the grand potential scales as $N_f(N_f + 1)/2$ at large N. So the quark-antiquark contributions to the thermodynamic observables are negligible with respect to the quark-quark and antiquark-antiquark ones in the 't Hooft limit.

Finally, using similar arguments, one can show that the contribution of the quark-gluon and antiquark-gluon interactions to the grand potential scale as $N_f N$ at large N. One concludes that in the 't Hooft large-N limit the grand potential is dominated by the gluonic contributions only, scaling as N^2.

V. PARAMETERS OF THE MODEL

A. Potential and gluon mass

Two ingredients are now missing to start numerical computations: the interaction potential between two gluons and the gluon mass. The procedure followed to fix the potential is similar to the one followed in Ref. [3] in the case of heavy quark-antiquark bound states. The first step is to take some input from lattice QCD, from which accurate computations of the static-free energy of a quark-antiquark pair bound in a color singlet, $F_1(r, T)$, are available. In particular, computations in quenched SU(3) lattice QCD can be found in Ref. [32]; they are especially relevant for our purpose since we focus on the pure Yang-Mills plasma. There is still debate on the proper potential term to use in phenomenological approaches, namely F_1 or the internal energy $U_1 = F_1 - T\partial_T F_1$. An entropic contribution is subtracted from the free energy in U_1, causing the internal energy to be more attractive than the free energy, eventually leading to larger dissociation temperatures for bound states in the deconfined medium. Spectral function analysis of heavy quarkonia from lattice QCD simulations of Euclidean correlation functions typically suggest that the η_c and J/ψ states may survive up to about $2\,T_c$. Such values of the dissociation temperature can be accommodated if the singlet internal energy is used in potential model calculations [33–36]. As in Ref. [3], the internal energy is used as a potential term. The explicit expression of the internal energy U_1 used in this work can be found in Appendix B.

The assumed color scaling (6) allows us to derive the two-gluon potential from the lattice quark-antiquark one. It is worth noting that a static potential is justified here because gluons acquire a mass within our approach. Given $U_1(r, T)$ computed in quenched SU(N) lattice data, the color factor of the singlet quark-antiquark pair reads

$$\kappa_{q\bar{q}} = -\frac{N^2 - 1}{2N^2}. \tag{44}$$

According to (6), the potential (in position space) between two quasigluons in the color channel $\mathcal{C}$ is then given by

$$V(r, T) = \frac{\kappa_{\mathcal{C};gg}}{\kappa_{q\bar{q}}}[U_1(r, T) - U_1(\infty, T)], \tag{45}$$

where the long-distance limit of the potential has to be normalized to zero in order to ensure the convergence of the scattering equation and to perform the Fourier transform. This is actually a standard procedure in finite-temperature calculations.

Moreover, according to the suggestion made in Ref. [37], the nonzero value of $U_1(\infty, T)$ should eventually be responsible for an effective in-medium contribution to the gluon mass. The intuitive argument is that when both gluons are infinitely separated, they no longer interact. Therefore, the remaining potential energy should be seen

as a manifestation of self-energy effects induced by the surrounding medium. These effects are encoded in the model as a mass shift to the "bare" quasigluon mass, whose value has still to be fixed. Since $U_1(\infty, T) = 2m_q(T)$, the adaptation to the gluon must be done by extracting the correct color dependence. From hard-thermal-loop (HTL) computations [38], the self-energy color dependence is given by C_2^q/C_2^{adj} at the first order when it is added in the propagator as a mass term (m^2), which means here that

$$\frac{U_1(\infty, T)}{2} = m_q(T) = \sqrt{\frac{C_2^q}{C_2^{\mathrm{adj}}}}\Delta(T). \tag{46}$$

So, $m_q(T) = 2\Delta(T)/3$ in the SU(3) case.

In the same way as for the two-body color scaling, $\Delta(T)$ is considered as universal and the gluon thermal mass reads

$$\delta(T) = \sqrt{\frac{C_2^g}{C_2^{\mathrm{adj}}}}\Delta(T) = \Delta(T), \tag{47}$$

since $C_2^g = C_2^{\mathrm{adj}}$. So, $\delta(T)$ is gauge-group independent. The effective in-medium gluon mass is finally given in our approach as

$$m_g(T)^2 = m_0^2 + \delta(T)^2, \tag{48}$$

where the value m_0 has still to be fitted (see the following section). All the contributions are quadratically added as is the case when one is dealing with bosonic propagators. The gluon mass is thus gauge-group independent. With lattice data taken from Ref. [32] (see Appendix B), its dependence on temperature is given in Fig. 1. As in standard quasiparticle approaches, the gluon mass is rising quite sharply when $T \longrightarrow T_c$ [39]. It is worth mentioning that in a recent work [40], it has been shown that the inclusion of a Polyakov loop dynamics leads to a gluon mass with a very smooth dependence on T. From HTL calculations, it is expected that at very high T, $m_g(T) \sim \sqrt{\alpha_S(T)}T$ [6,38], with a quasilinear behavior for $T \gtrsim 2\,T_c$. This is not the case in our model since our ansatz for the gluon mass is not inspired from HTL theory but is instead completely driven—with no freedom—by data from Ref. [32], limited to 3 T_c. It could be interesting if new data above this temperature were computed in order to confirm or infirm the decrease of $m_g(T)$. We will see in Sec. VII A that this behavior is not a problem for reproducing the pressure.

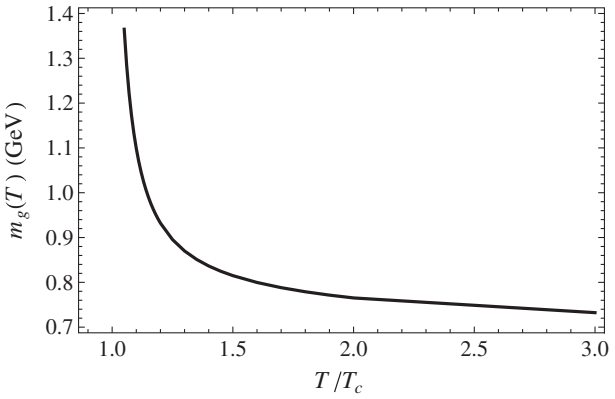

FIG. 1. Thermal gluon mass $m_g(T)$ in GeV, given by (48), as a function of the ratio T/T_c.

It is obvious that the problem of the gluon mass is far more complicated than the simple prescription (48), which has to be seen as valid in a first approximation only. A more refined gluon mass should probably be momentum dependent. There is indeed an increasing amount of evidence favoring the existence of a dynamically generated gluon mass due to nonperturbative effects, at least at zero temperature. Such a dynamically generated gluon mass $m_g(p)$, with $m_g(\infty) = 0$ and $m_g(0)$ finite, is favored by some lattice results in the Landau gauge, see e.g., Refs. [41,42]. Also nonperturbative field-theoretical calculations, using for example the pinch technique, find a nonzero dynamically generated gluon mass in $3+1$ Yang-Mills theory [43–45]. It is also worth quoting the recent Coulomb gauge study [46], which is a first step in view of understanding the behavior of $m_g(p, T)$ at a nonperturbative level. From a different perspective, nonperturbative contributions to the gluon potential and mass are analyzed at finite temperature in connection with the gluon condensates in Ref. [47]. Such improvements of the gluon mass are left for future works.

The above discussion gives a more precise meaning to the term "quasigluon" used in this paper: It denotes transverse particles in the adjoint representation of SU(N) that gain an effective mass $m_g(T)$ given by (48) and that interact through the potential (45).

B. Zero temperature results with SU(3)

Before performing finite-temperature computations, it is worth checking whether or not the values retained for the various parameters of our model may give relevant results at zero temperature. In particular, is the present T-matrix formalism able to reproduce, at least qualitatively, the features of the low-lying glueball spectrum computed in pure gauge SU(3) lattice QCD at zero temperature? [48]

It is known that at zero temperature and in quenched SU(3) lattice QCD, the potential between a static quark-antiquark pair is compatible with the funnel form [49]

$$V_f(r) = \sigma r - \frac{4}{3}\frac{\alpha}{r}. \tag{49}$$

In order to stay coherent with the potential above T_c, $\alpha = 0.141$ (see Appendix B) and $\sigma = 0.176$ GeV^2 (a standard value for the string tension) are used. The Fourier transform of $V_f(r)$ is not defined: This flaw can be cured by making it saturate at some value V_{sb}, interpreted as a string-breaking value, which is the energy above which a light quark-antiquark pair can be created from the vacuum and

break the QCD string. This scale is then subtracted and the potential effectively taken into account is $V_f(r) - V_{\rm sb}$, while $V_{\rm sb}$ is interpreted as an effective quark mass using the same arguments as those detailed in Sec. VA. According to the color scaling (7), the potential that should be used to describe the interactions between two gluons at zero temperature is

$$V_0(r) = \frac{9}{4} V_f(r) - V_{sb}^g \tag{50}$$

when the gauge group is SU(3). In this case, the string-breaking scale should rather be interpreted as the energy scale necessary to form two gluelumps, a gluelump being a gluon bound in the color field of a static adjoint source. It is known indeed that adjoint string breaking may be observed and occurs at twice the lightest gluelump mass (~ 2 GeV) [50]. So, $V_{\rm sb}^g = 2$ GeV is used here, a value in agreement with lattice data showing that the mass of the lightest gluelump is given by 0.85(17) GeV [51].

The only free parameter left to compute the T matrix is the bare gluon mass, m_0. Keeping the same structure as in Eq. (48), we have

$$m_g(0)^2 = m_0^2 + \left(\frac{V_{\rm sb}^g}{2}\right)^2, \tag{51}$$

where again we have traded the subtracted potential at infinite separation distance (string breaking energy in this case) into a self-energy-like contribution to the quasiparticle gluon mass. We fix $m_0 = 0.7$ GeV, which is an acceptable value for the zero-momentum limit of the gluon propagator at zero temperature in view of previous studies, locating this mass typically between 500 and 700 MeV, see e.g., Refs. [42,43,52]. Advancing results, such a value will ensure both a correct agreement with the zero temperature lattice glueball spectrum (see Table II) and an excellent agreement with the pure gauge EoS computed on the lattice (see Sec. VII A).

The results are given in Table II for J^P channels discussed in Sec. III B. Let us first focus on the fourth column, corresponding to our initial set of parameters. At least, in this case, our model is able to reproduce the mass hierarchy of the lightest glueballs observed in lattice QCD, as well as the typical mass scale of 2 GeV for those states. The accuracy of the model can be compared to Coulomb gauge QCD (CGQCD) [52], sharing formally many similarities with our T-matrix approach. The results of this last reference are also given in Table II. The agreement between lattice QCD and Coulomb gauge is better, but it is worth saying that the parameters used in CGQCD have been chosen to reach an optimal agreement with the zero temperature lattice data, while here the values are mostly designed to give good results above T_c.

TABLE II. Masses (in GeV) of the lowest-lying glueball states at zero temperature with the gauge group SU(3). Our results (fourth and fifth columns) are compared to the lattice data of Morningstar and Peardon [48] (second column) and to the Coulomb gauge QCD (CGQCD) study [52] (third column). The fourth column is a T-matrix calculation with the value $\alpha = 0.141$, while the value $\alpha = 0.4$ is taken in the last column to include running coupling effects.

State	Lattice [48]	CGQCD [52]	T matrix $\alpha = 0.141$	T matrix $\alpha = 0.4$
0^{++}	1.73 (5)(8)	1.98	2.17	1.96
0^{-+}	2.59 (4)(13)	2.22	2.39	2.26
2^{++}	2.40 (2.5)(12)	2.42	2.34	2.21

What makes us find such a high mass for the scalar glueball is the quite small value $\alpha = 0.141$ that has been taken (in order to fit static potentials above T_c), while values as high as $\alpha = 0.4$ have sometimes to be used to reach a good agreement between lattice data and effective approaches, see e.g., Ref. [22]. The scalar glueball being dominantly an S-wave state, it should be particularly sensitive to the strength of the Coulomb term and to a possible running of α with the temperature. The existence of such a running coupling with the temperature is well known, see e.g., the pioneering work [53], where $\alpha(T)$ follows from standard renormalization arguments, with the temperature playing the role of the energy scale. Although to our knowledge no definitive conclusion can be drawn yet, it is tempting to assume that $\alpha(0)$ is finite and larger than $\alpha(T > T_c)$. Fits on the lattice static potential in Ref. [32] actually favor such a saturation at zero temperature. Assuming that $\alpha(0) = 0.4$ due to running effects actually improves the agreement between our model and lattice data, as can be seen in the last column of Table II. Our results then become nearly equivalent to those of CGQCD. Note that, in the rest of this paper, we will focus on the temperature interval (1–4) T_c in which the running of α can be neglected as confirmed by the quality of the fit on the lattice data with the single value $\alpha = 0.141$. Let us note also that the discrepancies between our results and those from the lattice for scalar and pseudoscalar states can also be partly due to the existence of a strong instanton interaction [22] not taken into account here.

Finally, the extension of the above calculations to any gauge group is straightforward in our approach since $\kappa_\bullet = -1$ for all gauge groups. The interested reader will find a discussion of such a generalization in Ref. [29], where it is shown that the lowest-lying glueball masses are gauge-group independent within a constituent framework. In particular, the lowest-lying glueball masses are found independent of N in Ref. [29], in agreement with what is observed on the lattice [54]. That is why the T-matrix masses given in Table II are considered as valid for any gauge group too.

C. Relevance of the parameters for other gauge groups

At this stage, it is important to summarize the various parameters introduced and their possible dependence—or

not—on the gauge group. Comparison with existing results when it is possible can also shed light on that issue.

First of all, the basic ingredient underlying the present study is the static quark-antiquark potential computed in finite-temperature quenched lattice QCD. The assumed one-gluon-exchange nature of the two-particle interactions leads to the universality of the momentum-dependent part of the potential and to a well-defined prescription for its gauge-group dependence. Similarly, the gluon thermal mass has a peculiar color scaling originating in its interpretation as a self-energy term.

More freedom is apparently left for the numerical parameters at our disposal. Let us comment on them briefly. First, the propagator imaginary part Σ_I has been introduced for computational convenience. Hence, it can be kept constant when changing the gauge group. Second, by dimensional analysis, it can be checked that our results can all be expressed in terms of the ratios T/T_c, $T_c/\sqrt{\sigma}$ and $m_0/\sqrt{\sigma}$.

According to glueball gas models with a Hagedorn spectrum describing the high-lying glueball states, the critical temperature is given by [26,55]

$$\frac{T_c}{\sqrt{\sigma}} = \sqrt{\frac{3}{2\pi}} = 0.69. \tag{52}$$

This value is due to the Hagedorn spectrum, not defined above a certain temperature. This temperature is here interpreted as the deconfinement one. It is worth noting that it leads to an EoS in very good agreement with lattice results [26,55,56] below T_c. In this picture, the ratio $T_c/\sqrt{\sigma}$ is gauge-group independent: This is only valid in a first approximation, since, for example, there is lattice evidence showing that $T_c/\sqrt{\sigma}$ is only constant up to $1/N^2$ corrections [57]. Nevertheless, such deviations are beyond the scope of this exploratory work. Note that according to Braun *et al.* [58], the critical temperature is found to be pretty close to 300 MeV up to a fluctuation of about 10% for the gauge groups SU(N), Sp(2), and E_7. So, we fixed $T_c = 300$ MeV in our calculations. This value is in good agreement with (52) for the value $\sigma = 0.176$ GeV^2 chosen for $T = 0$ calculations (see Sec. V B).

Concerning the ratio $m_0/\sqrt{\sigma}$, it is worth mentioning the work [59], in which it is shown that the nonperturbative gluon propagator at zero temperature (m_0, in particular) shows no significant quantitative differences when expressed in units of the string tension for the groups SU(N) and G_2. It is thus tempting to say that the ratio $m_0/\sqrt{\sigma}$ may be gauge-group independent also. This is assumed in the rest of this paper. The value $m_0/\sqrt{\sigma} = 1.67$ obtained from the zero-temperature glueball spectrum is retained.

Finally, let us finally mention that, at zero temperature, the string-breaking scale is found to be two times the glueball mass for SU(N) and G_2 [28]. This means that the extension of the above zero-temperature calculations to any gauge group is straightforward in our approach. The T-matrix masses given in Table II can be considered as valid for any gauge group once divided by $\sqrt{\sigma}$.

VI. EXISTENCE OF GLUEBALLS ABOVE T_c

A. Singlet states

Now that all the parameters of the model have been fixed, T-matrix calculations above T_c can be performed. Technical details will not be given here, since the method is identical to the one used in Ref. [3], which involves the Haftel-Tabakin algorithm to solve the T-matrix Lippmann-Schwinger equation [25]. The bound and resonant states appear as poles in the on-shell T matrix or, more precisely, as zeros of $\det \mathcal{F}$. The corresponding masses are given in Table III in the different considered color-singlet channels. Since in this case, $\kappa_{\mathrm{C};\bullet} = -1$ for all gauge groups and since the gluon mass is independent of N, the masses of the color-singlet are the same for SU(N) for all N and for G_2.

Only a few papers devoted to the existence of glueballs on the lattice are currently known [60,61], and the interpretation of their results depends mostly on the way the glueball correlators are fitted—with either a single narrow

TABLE III. Masses (in units of $\sqrt{\sigma}$) of lowest-lying glueballs above T_c ($T_c = 0.3$ GeV). Dots mark the temperature at which a bound state is not detected anymore.

Channel			Singlet			Adjoint^S			$(2,0)^S$		
Group			All			SU($N \geq 3$)			G_2		
T/T_c	$2\,m_g$	0^{++}	0^{-+}	2^{++}	0^{++}	0^{-+}	2^{++}	0^{++}	0^{-+}	2^{++}
1.05	6.50	4.52 6.48[a]	5.43	5.43	6.00	6.45	6.31	6.14	…	6.38
1.10	5.24	4.57	5.21	5.00	5.14	…	…	5.21		…
1.15	4.71	4.43	…	4.67	…			…		
1.20	4.43	4.33		…						
1.25	4.26	4.24								
1.30	4.14	…								
1.35	…									

[a]Radial excitation below the threshold.

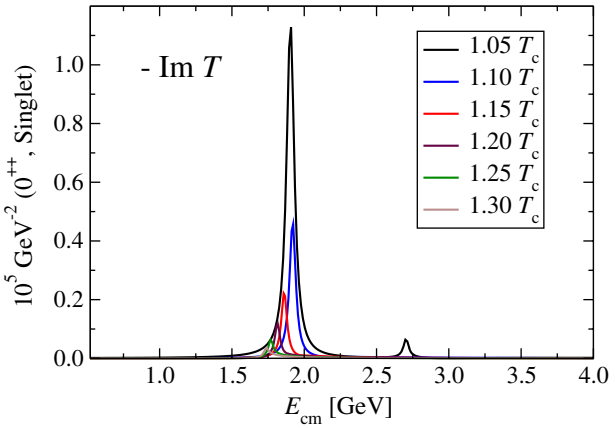

FIG. 2 (color online). ImT for gg scattering in the 0^{++} singlet channel for various T with $T_c = 0.3$ GeV. The peak position decreases with increasing temperature.

pole or a Breit-Wigner shape. Let us focus on the narrow pole fit, which identifies bound states in a way similar to ours. The main observation to be made from Refs. [60,61] is that the glueball masses decrease above T_c with increasing temperature, with a mass near T_c that is similar to the zero temperature one. This nontrivial behavior is well checked within our approach. Two competing effects are responsible for the temperature evolution of the spectrum: reduction of the binding energy and downward shift of the threshold energy due to the decrease of the gluon mass. Overall, the singlet scalar bound state experiences a mild shift to lower energies and dissociates at $T_{\rm dis} \approx 1.3\,T_c$. This is the value from which $\det \mathcal{F}$ does not vanish anymore. Nevertheless, considerable strength remains at threshold up to about 1.5 T_c. This is in qualitative agreement with the spectral function analysis of Euclidean correlators by the CLQCD Collaboration [61].

The evolution of the imaginary part of the on-shell T matrix in the singlet scalar channel versus the temperature is displayed in Fig. 2: This gives an overall picture of the glueball progressive dissolution in the medium. The peak in the imaginary part, depicting a bound state, becomes broader and broader before melting into the continuum (and thus $\det \mathcal{F}$ does not vanish anymore below threshold) as the temperature is increased. Still, for $T > T_{\rm dis}$ and above the threshold energy, one finds sizable strength from the bound state relic, the T matrix exhibiting a resonant behavior well beyond the Born approximation.

Concerning the pseudoscalar channel, singlet bound states are found up to 1.10 T_c. Note that states in the pseudoscalar channels, which in our approach correspond to pure P-wave scattering, are just mildly bound due to the centrifugal barrier. The tensor states, having an S-wave component, lie between the scalar and pseudoscalar channels, regarding binding and dissociation temperatures.

B. Colored states

Bound states in the symmetric adjoint channel of SU($N \geq 3$) are also observed (see Table III), although they are less bound since $\kappa_{\mathcal{C};\bullet} = -1/2$. The scalar channel disappears above 1.10 T_c, whereas in the pseudoscalar and tensor channels, bound states are lying right below the threshold energy at the lowest considered temperature (i.e., 1.05 T_c). The differences between singlet and adjoint channels have to be attributed to the strength of

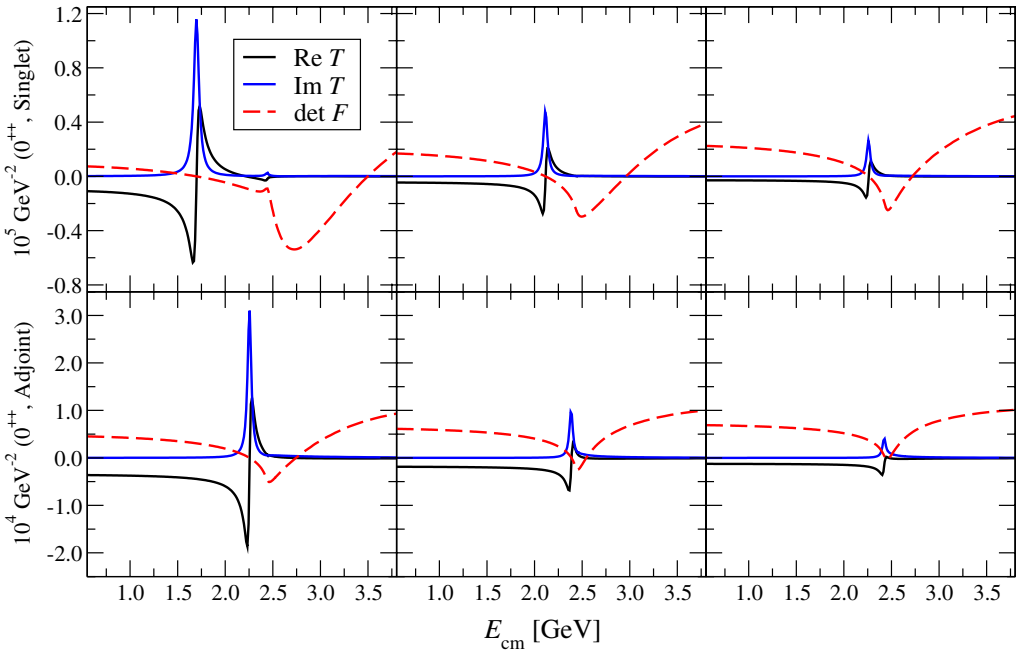

FIG. 3 (color online). T matrix for gg scattering in the scalar singlet and scalar symmetric adjoint channels for SU($N \geq 3$). From left to right, the temperatures are (1.05; 1.10; 1.15) T_c, with $T_c = 0.3$ GeV.

the potential, which is two times smaller in the adjoint channel than in the color singlet.

The evolution of the T matrix in the singlet and symmetric adjoint scalar channel versus the temperature is displayed in Fig. 3. One clearly sees the disappearance of this bound state at 1.15 T_c, while the singlet state is still well bound at this temperature.

There are, in general, other colored channels than the adjoint one. For SU(N) gauge groups, in particular, the only one that could *a priori* lead to bound states is the $(0, 1, 0, \ldots, 0, 1, 0)^S$ channel, which is weakly attractive and exists only for $N > 3$. It has been checked that even the scalar state (the most attractive channel) is unbound at $N = 4$. Hence, this color channel does not admit bound states. In the case of G_2, the other group considered in this study, the $(2, 0)^S$ channel leads to bound states with the same melting temperatures as in the adjoint channel, up to our current precision of 0.05 T_c (see Table III).

VII. EQUATION OF STATE

The pure gauge EoS can now be computed without introducing extra parameters: The two-body potential and the thermal mass contribution to the gluon mass have been fitted on lattice data by using, respectively, the scaling (45) and (47), and they ensure a correct agreement with zero temperature results. A crucial point in establishing the EoS, thanks to (15), is correctly expressing the summation on the different channels. For 2-gluon interactions, the channels are cued by the J^P number and the color number. The summation on the J^P channels is formally infinite, but in this work, only the 0^{++}, 0^{-+}, and 2^{++} channels are taken into account. This restriction is supported by the following argument. These three channels are the most attractive ones and generate the lightest glueballs. The lighter the mass, the more important the thermodynamic contribution is in the bound state sector. Thus, the bound state thermodynamic contribution coming from other J^P should be negligible in comparison to these three channels. In order to be coherent, this J^P restriction is implemented in the scattering sector. It also creates a restriction in the allowed color channels. Since the 0^{++}, 0^{-+}, and 2^{++} are symmetric J^P channels, the color channels must be symmetric too in order to respect the Pauli principle.

A. Pressure

In Fig. 4, the normalized pressure p/p_{SB} obtained by our approach in the SU(3) case is compared with the normalized pressure computed in the free gluon gas case for the thermal mass (48) and with the bound states and scattering contributions. The situation is similar for the other gauge groups. At low temperature ($T \leq 1.3\,T_c$), the bound states and the scattering parts both give thermodynamic contributions that modify the free gas pressure, but the effect of the bound states is very small. For $T > 1.3\,T_c$, only the scattering part contributes. As can be observed in Fig. 4,

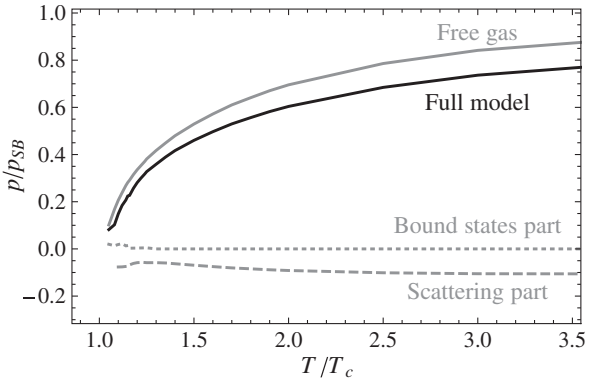

FIG. 4. Normalized pressure p/p_{SB} versus temperature in units of T_c (with $T_c = 0.3$ GeV), computed for the gauge group SU(3) in the free gluon gas case and in the full approach. The bound states and scattering contributions are also indicated. The black curve is the sum of the gray curves.

the main global effect of the interaction, resulting from the combination of various positive and negative contributions, is a decrease in the pressure. In our model then, this decrease is not caused by an increase of the thermal gluon mass at high T (see Sec. V A). The data extracted from the lattice QCD [32] give a coherent picture of the thermodynamic behavior: the interactions compensate for the decrease of the thermal gluon mass.

If each contribution is analyzed, it is seen that the bound state formation increases the pressure because bound states are simply added as new species that do not interact with the other particles inside the plasma. With a glueball melting into the plasma for a given temperature T_{dis}, its contribution to the pressure disappears abruptly for $T = T_{\mathrm{dis}}$. As the global effect of bound states is very small, this situation is not really disturbing. It is more problematic for the computation of other observables, as we will see in the next section.

Concerning the two-gluon scattering part, the sign of the pressure contribution cannot be analytically predicted at each temperature. Only at the Born approximation one can observe that attractive (repulsive) channels contribute to increase (decrease) the pressure. Indeed, in momentum space representation (see Appendix C), (10) becomes here

$$\Omega_s = \frac{1}{64\pi^5\beta}\sum_{J^P}(2J+1)\sum_{\mathcal{C},g}\dim\mathcal{C}\,\kappa_{\mathcal{C},gg} \times \int_{2m_g}^{\infty} d\epsilon\,\epsilon^3\sqrt{\frac{\epsilon^2}{4}-m_g^2}\,K_1(\beta\epsilon)\,v_{J^P}, \tag{53}$$

where $K_1(x)$ is the modified Bessel function of the first kind. In the attractive (repulsive) channels, the sign of the potential is negative (positive). Since Ω_s is the scattering contribution to the grand potential, it can be deduced that attractive (repulsive) channels increase (decrease) the pressure. In the present SU(3) case, the only repulsive channel

is the $(2,2)^S$. This means that the decreasing of the pressure in our approach, compared with the free gas pressure, is only driven by the $(2,2)^S$ channel.

It is also worth wondering whether or not some constraints arise from the high-temperature limit of our framework concerning the behavior of the two-body interactions. In this limit, the Born approximation should be relevant. Using (38) and (53), one can write

$$\Omega_s \sim \frac{1}{64\pi^5\beta}\frac{\dim \mathrm{adj}}{2}\int_{2m_g}^{\infty} d\epsilon\epsilon^3\sqrt{\frac{\epsilon^2}{4}-m_g^2}K_1(\beta\epsilon)v_0. \quad (54)$$

Only the scalar channel has been taken into account for the sake of clarity, but the following argument can be extended to any spin. According to HTL results, it is relevant to assume a Yukawa form for the potential v_0 at high temperature [38]. Then,

$$\Omega_s \sim \frac{1}{64\pi^5\beta^4}\frac{\dim \mathrm{adj}}{2}\int_{2\beta m_g}^{\infty} dx x^3 K_1(x) \times \frac{\sqrt{\frac{x^2}{4}-\beta^2 m_g^2}}{\frac{x^2}{4}-\beta^2 m_g^2-\beta^2 M^2}, \quad (55)$$

where M is the screening mass of the theory, *a priori* temperature dependent. Still, in HTL theory, it is found that because of the running of the strong coupling constant,

$$\lim_{\beta\to 0}\beta m_g = \lim_{\beta\to 0}\beta M = 0. \quad (56)$$

More precisely, the quark and gluon thermal masses are found to behave as $\sqrt{\alpha_s(T)}T$. Consequently, at high enough temperatures, it is found that

$$\Omega_s \sim \frac{\dim \mathrm{adj}}{32\pi^5\beta^4}, \quad (57)$$

i.e., a scattering contribution that has the same behavior with respect to the temperature as the free part, ensuring a well-defined large-temperature limit. Notice that our fit of the screening mass does not follow the constraints (56) but is designed to fit the static potential below 3 T_c. A more involved form would be needed to reach the HTL predictions at high temperatures, but it is not in the scope of the present work.

In Fig. 5, the normalized pressure p/p_{SB} is presented for different gauge groups: SU(2), SU(3), SU(∞), and G_2. Several remarks can be made. First, the free-gluon thermodynamic contribution is gauge-group invariant once normalized to p_{SB}. The gauge-group dependence is only present in the bound state and scattering sectors. The number of allowed color channels (i.e., the symmetric ones) depends on the gauge group [see (33)] and determines the allowed maximum number of bound states and the number of scattering channels. Note that the small bound state thermodynamic contribution comes from two effects—the number and mass of the existing glueballs.

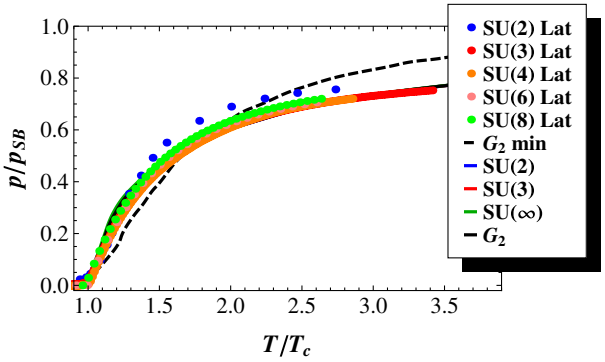

FIG. 5 (color online). Normalized pressure p/p_{SB} versus temperature in units of T_c (with $T_c = 0.3$ GeV), computed for the gauge groups SU(2, 3, ∞) and G_2 (solid lines). Note that all the curves are nearly indistinguishable. Our results are compared to the lattice data of Engels *et al.* [68] for SU(2) (dots) and Ref. [62] for SU(3, 4, 6, 8) (dots), and of the minimal G_2 model of Dumitru *et al.* [64] for G_2 (dashed line). Note that all lattice data have been normalized to the lattice Stefan-Boltzmann pressure [62,68].

Because of the glueball dissociation, this contribution is only taken into account up to the temperature of dissociation (see Table III). One can observe in Fig. 5 that the produced EoS is not very sensitive to the gauge group. The most important difference between the curves occurs between 1.05 and 1.35 T_c (see Fig. 6). In this range, the gluon-gluon interactions are maximal. When the temperature increases, the Born approximation becomes more and more valid and the pressure then scales as dim adj. Thus the normalized pressure tends to be universal.

In Fig. 5, it is also worth noticing that the EoS computed in our approach favorably compares with QCD lattice data for gauge groups SU(3–8) [62], where such universal curves seem to appear (note that lattice data exist also for very high values of T/T_c but only for SU(3) [63]). Concerning G_2, no lattice data about EoS are currently

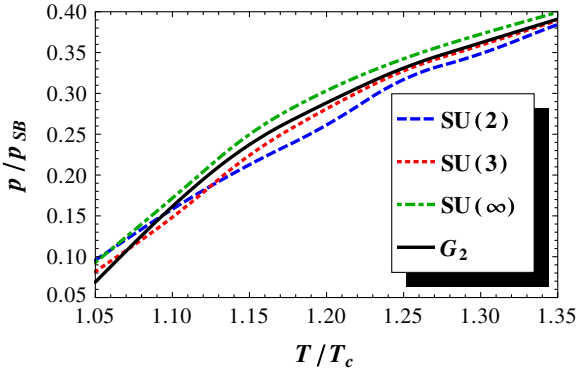

FIG. 6 (color online). Normalized pressure p/p_{SB} versus temperature in units of T_c (with $T_c = 0.3$ GeV), computed for the gauge groups SU(2), SU(3), G_2, and SU(∞). The temperature range is the one where the differences between the curves are the most important.

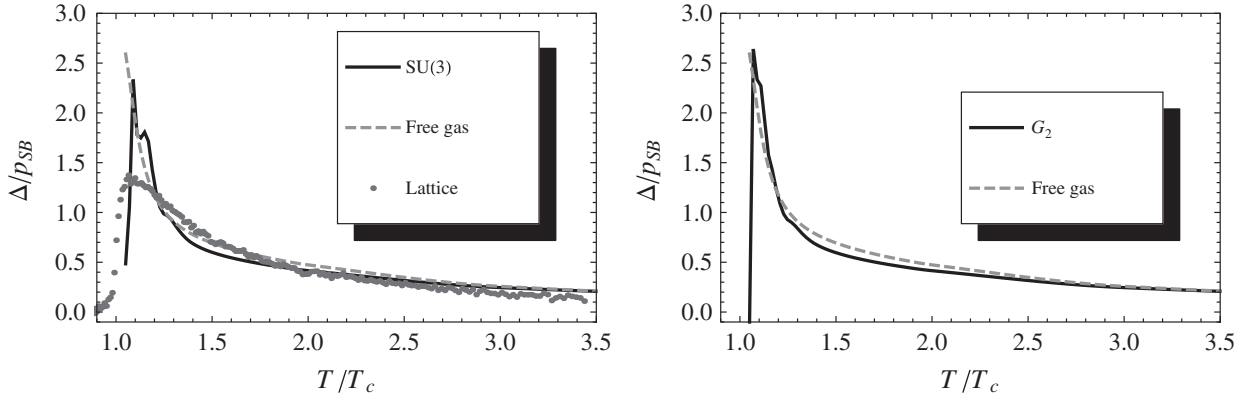

FIG. 7. Normalized trace anomaly Δ/p_{SB} versus temperature in units of T_c (with $T_c = 0.3$ GeV) computed for the gauge groups SU(3) (left) and G_2 (right). The models (black solid line) are compared with the free gas (dashed grey line) and the lattice data from Ref. [62] in the SU(3) case (dark grey dots).

available, but a new effective matrix model describing pure Yang-Mills thermodynamics has been proposed in Ref. [64]. These last results are compared to ours in Fig. 5.

B. Trace anomaly

A relevant observable that measures the nonideal character of the deconfined medium is the trace anomaly $\Delta = e - 3p$, where e is the energy density. We have computed this quantity in the framework of our model, but the results obtained can only be considered as preliminary for the two reasons explained below.

In principle, the trace anomaly can be computed from the pressure thanks to the thermodynamic relations. As the Hamiltonian considered explicitly depends on the temperature, these relations must be used with some caution. For instance, in the case of free particles with a temperature-dependent dispersion relation, several procedures exist to compute the observables, keeping the usual thermodynamic relations [5,16]. With temperature-dependent mass and interactions as in our model, all observables obtained by derivation of the grand potential must be examined with caution. Here, we will simply use the usual relation

$$\frac{\Delta}{p_{\mathrm{SB}}} = -\beta\left(\partial_\beta \frac{p}{p_{\mathrm{SB}}}\right)_{\beta\mu}, \tag{58}$$

but a self-consistent procedure is needed.

As mentioned in the previous section, the glueball contributions to the pressure disappear abruptly at the melting temperature. The derivative of the pressure for this temperature is then not defined. At first sight, one could argue that the contribution of the glueballs to the pressure is so weak that it can be safely neglected. But, this does not mean a small contribution to the derivative of the pressure. Moreover, the glueballs exist in a domain of temperature, where the deviation from the nonideal character of the gluon plasma is expected to be large. Thus, a smooth transition between a bound state with a finite width and a scattering state of two gluons is worthwhile. It could be obtained by a unified treatment of the T-matrix results in the computation of the grand potential. This would imply a strong modification of the formalism developed in Ref. [4]. Here, we will simply not take into account the glueball contributions in (58), leaving a detailed study for another work.

The normalized trace anomaly computed with (58) for SU(3) and G_2, without the bound state contributions, are compared in Fig. 7 with the (gauge-independent) normalized trace anomaly computed for the free gluon gas with the thermal mass (48) and with the lattice data from Ref. [62] in the SU(3) case. The G_2 trace anomaly, like the pressure, is not significantly different from its SU(3) counterpart. The situation is similar for the other gauge groups. The peak near T_c results from the combination of various negative and positive channel contributions. This explains its nonstandard structure. One can see that this peak is not in good agreement with the lattice data. This discrepancy could be cured by a correct treatment of the bound state contributions and melting, as well as by a self-consistent computation of this observable. However, the peak cannot be obtained with the free part only and the behavior above 2 T_c is in agreement with lattice data. These are probably the most important features of our model concerning the trace anomaly. Improved calculations are necessary to clarify the situation.

VIII. CONCLUSIONS

The relevance of gluon-gluon interactions beyond the critical temperature in the pure gauge SU(3) plasma has been addressed in a nonperturbative T-matrix many-body framework with the input of Casimir-scaled potentials from thermal lattice QCD and a model of quasigluon mass independent of the gauge group. Scalar glueball bound states in the singlet channel survive up to temperatures of about (1.3–1.5) T_c, together with sizable threshold effects due to strong correlations beyond the two-particle threshold. This fast melting of glueballs is in agreement

TABLE IV. Symmetry, dimension ($\dim \mathcal{C}$), and color factor ($\kappa_{\mathcal{C}}$) defined in (32) of the color channels ($\mathcal{C}$) appearing in the tensor product of the SU(N) adjoint representation by itself. This table actually displays the two-gluon color channels, denoted by gg. The SU(3) case is also indicated.

$\mathcal{C}$ for gg	•	$(1,0,\ldots,0,1)$	$(2,0,\ldots,0,2)$,	$(2,0,\ldots,1,0)$, $(0,1,\ldots,2)$	$(0,1,0,\ldots,0,1,0)$
SU(3)	•	(1, 1)	(2, 2)	(3, 0), (0, 3)	$\cdots$
Symmetry	S	S, A	S	A	S
$\dim \mathcal{C}$	1	N^2-1	$\frac{N^2(N+3)(N-1)}{4}$	$\frac{(N^2-4)(N^2-1)}{4}$	$\frac{N^2(N-3)(N+1)}{4}$
$\kappa_{\mathcal{C}}$	-1	$-\frac{1}{2}$	$\frac{1}{N}$	0	$-\frac{1}{N}$

with the results of a recent Coulomb gauge Yang-Mills theory at finite temperatures [65]. With only one free parameter, the gluon mass at $T=0$, the EoS of the gluon-glueball gas is reproduced in good agreement with quenched lattice SU(N) simulations (the other parameters can be fixed *a priori* by resorting to either lattice results or theoretical arguments). Predictions for the G_2 EoS are also given, with results very close to the SU(N) ones once normalized to the Stefan-Boltzmann pressure. The main result of this work is that though the pressure of the gluon plasma is mainly due to the thermal mass, the scattering term provides a mild but necessary contribution to fit the data, the bound state contributions being completely negligible. Moreover, the scattering contributions are responsible for the sharp peak of the trace anomaly near T_c.

The present T-matrix formalism can, in principle, be systematically improved, for example, by the inclusion of quasiparticle self-energy effects through a self-consistent formalism. A unified description that places on an equal footing the scattering and bound states is also worthwhile to allow a coherent computation of other observables. Another natural extension to this paper is to study the light meson spectrum at finite temperature and the QCD EoS by including quarks within the model. Computations with baryonic potential can be considered also.

The T-matrix formalism also can be applied to calculate bulk thermodynamic properties of the system, such as the sheer viscosity, which can be easily computed in relaxation-time approximation within a quasiparticle picture. Such a work is in progress.

Finally, the inclusion of three-gluon scattering is also possible but much more involved. The number of channels under consideration is quite large compared with the two-gluon case, with more elaborated symmetries. Moreover, finding the T matrix would then become a three-body problem, whose resolution through e.g., Faddeev equations can be addressed in future works.

ACKNOWLEDGMENTS

This work has been partly supported by Grant No. FPA2011-27853-C02-02 (Ministerio de Economía y Competitividad, Spain). D. C. acknowledges financial support from Centro Nacional de Física de Partículas, Astropartículas y Nuclear (CPAN, Consolider—Ingenio 2010). G. L. and C. S. thank F.R.S-FNRS for financial support. The authors thank M. Panero for useful comments.

APPENDIX A: SOME SU(N) RELATIONS

The dimensions of the color channels appearing in (33) are given in Table IV, together with the color factors (32). Note that a general method for computing the quadratic Casimir of SU(N) can be found in Ref. [66].

Similar results can be written in the case where only the fundamental and/or conjugate representations are taken into account. The terms appearing in the tensor product of the fundamental and conjugate representations by themselves are given in Table V, as well as those appearing in the tensor product of the fundamental representation by the conjugate one.

TABLE V. Symmetry, dimension ($\dim \mathcal{C}$), and color factor ($\kappa_{\mathcal{C}}$) defined in (7) of the color channels ($\mathcal{C}$) appearing in the tensor product of the SU(N) fundamental representation by itself (left), of the conjugate representation by itself (middle), and of the fundamental representation by the conjugate one (right). This table actually displays the quark-quark, antiquark-antiquark, and quark-antiquark color channels, denoted by qq, $\bar{q}\,\bar{q}$, and $q\bar{q}$, respectively.

	qq		$\bar{q}\,\bar{q}$		$q\bar{q}$	
$\mathcal{C}$	$(2,0,\ldots,0)$	$(0,1,0,\ldots,0)$	$(0,\ldots,0,2)$	$(0,\ldots,0,1,0)$	•	$(1,0,\ldots,0,1)$
Symmetry	S	A	S	A		
$\dim \mathcal{C}$	$\frac{N(N+1)}{2}$	$\frac{N(N-1)}{2}$	$\frac{N(N+1)}{2}$	$\frac{N(N-1)}{2}$	1	N^2-1
$\kappa_{\mathcal{C}}$	$\frac{N-1}{2N^2}$	$-\frac{N+1}{2N^2}$	$\frac{N-1}{2N^2}$	$-\frac{N+1}{2N^2}$	$-\frac{N^2-1}{2N^2}$	$\frac{1}{2N^2}$

TABLE VI. Dimension ($\dim \mathcal{C}$) and color factor ($\kappa_{\mathcal{C}}$) defined in (7) of the color channels ($\mathcal{C}$) appearing in the tensor product of the SU(N) fundamental representation by the adjoint one (left) and of the conjugate representation by the adjoint one (right). This table actually displays the quark-gluon and antiquark-gluon color channels, denoted by qg and $\bar{q}g$, respectively.

		qg			$\bar{q}g$	
$\mathcal{C}$	$(1,0,\ldots,0)$	$(2,0,\ldots,0,1)$	$(0,1,\ldots,0,1)$	$(0,\ldots,0,1)$	$(1,0,\ldots,0,2)$	$(1,0,\ldots,1,0)$
$\dim \mathcal{C}$	N	$\frac{(N+2)N(N-1)}{2}$	$\frac{(N+1)N(N-2)}{2}$	N	$\frac{(N+2)N(N-1)}{2}$	$\frac{(N+1)N(N-2)}{2}$
$\kappa_{\mathcal{C}}$	$-\frac{1}{2}$	$\frac{1}{2N}$	$-\frac{1}{2N}$	$-\frac{1}{2}$	$\frac{1}{2N}$	$-\frac{1}{2N}$

Finally, useful results concerning the tensor product of the fundamental (conjugate) representation by the adjoint representation are given in Table VI.

APPENDIX B: LATTICE POTENTIAL

The lattice data that are used as a starting point to build our interaction potential are those of Kaczmarek *et al.* [32], i.e., the static-free energy between a quark-antiquark pair bound in a color singlet for $N = 3$. For numerical convenience, it is preferable to deal with a fitted form of these, rather than with interpolations of the available points. To fit the data of Kaczmarek *et al.* [32], the analytic form proposed by Satz in Ref. [67] is used,

$$F_1(r,T) = \frac{\sigma}{\mu(T)}\left[\frac{\Gamma(1/4)}{2^{3/2}\Gamma(3/4)} - \frac{\sqrt{\mu(T)r}}{2^{3/4}\Gamma(3/4)}K_{1/4}(\mu(T)^2r^2)\right] - \frac{4}{3}\frac{\alpha}{r}[e^{-\mu(T)r} + \mu(T)r]. \quad \text{(B1)}$$

The following explains how to obtain this formula. First, it is known that the static quark-antiquark energy at zero temperature is accurately fitted by a so-called funnel shape,

$$F_1(r,0) = \sigma r - \frac{4}{3}\frac{\alpha}{r} = U_1(r,0), \quad \text{(B2)}$$

see e.g., Ref. [49]. When $T > 0$, one can imagine that this potential is progressively screened by thermal fluctuations.

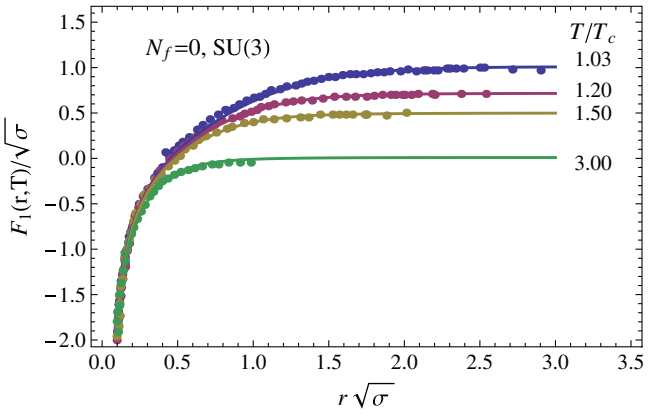

FIG. 8 (color online). Static-free energy $F_1(r,T)$ of a quark-antiquark pair bound in a color singlet, computed in SU(3) quenched lattice QCD and plotted for different temperatures (symbols). Data are taken from Ref. [32] and expressed in units of $\sqrt{\sigma}$, with r the quark-antiquark separation. The fitted form (B1)–(B4) is compared to the lattice data (solid lines).

An effective theory for studying the screening of a given potential is the Debye-Hückel theory, in which the thermal fluctuations are all contained in a screening function $\mu(T)$, which modifies the zero-temperature potential and eventually leads to the form (B1).

The explicit form of $\mu(T)$ is unknown *a priori* and has to be fitted on the lattice data. As can be seen in Fig. 8, the form

$$\frac{\mu(T)}{\sqrt{\sigma}} = 0.537\frac{T}{T_c} + 0.644 + 0.112\ln\left(\frac{T}{T_c} - 0.967\right), \quad \text{(B3)}$$

with

$$\alpha = 0.141, \quad \text{(B4)}$$

provides an accurate fit of the lattice data in the range 1–3 T_c. A more complete fit should be such that $\mu(0) = 0$, but our model is not intended to be able to "cross" the phase transition in T_c. The simple form (B3) is already satisfactory. The corresponding internal energy $U_1 = F_1 - T\partial_T F_1$ is plotted in Fig. 9.

APPENDIX C: DASHEN, MA, AND BERNSTEIN'S FORMALISM IN MOMENTUM SPACE

To compute (15), it is necessary to use a given representation. In order to use the calculation of the T matrix proposed in Ref. [3], the scattering part of (10) must be computed in the momentum space representation (the two first terms are simply free gas contributions and can be easily computed). Let us focus on

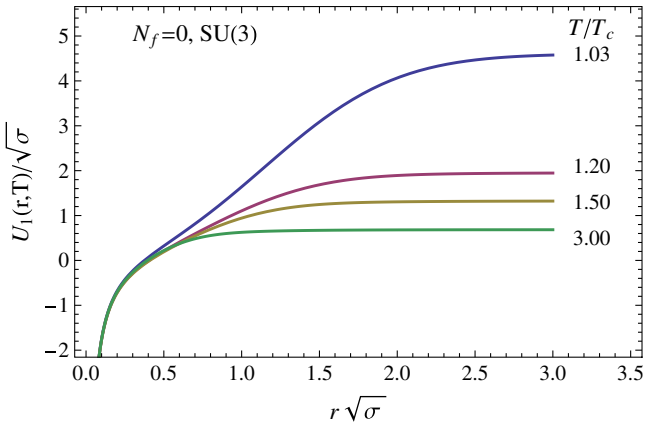

FIG. 9 (color online). Internal energy $U_1(rT)$ of a quark-antiquark pair bound in a color singlet, computed from the fitted form (B1)–(B4) and plotted for different temperatures (solid lines).

$$\Omega_s = \sum_{\mathcal{C}} \sum_{J^P} \frac{\dim \mathcal{C}}{2\pi^2 \beta^2} (2J+1) \int_{2m_g}^{\infty} d\epsilon \epsilon^2 K_2(\beta\epsilon) \times \mathrm{Tr}_{\mathcal{C},J^P}[(\delta \,\mathrm{Re}\mathcal{T})' - 2\pi((\delta \,\mathrm{Re}\mathcal{T})(\delta \,\mathrm{Im}\mathcal{T})' - (\delta \,\mathrm{Im}\mathcal{T})(\delta \,\mathrm{Re}\mathcal{T})')]. \quad \text{(C1)}$$

Using the following definitions concerning the trace of an operator A in momentum space,

$$\mathrm{Tr}\, A = \frac{1}{(2\pi)^3} \int_{-\infty}^{\infty} d\vec{q} \langle \vec{q}|A|\vec{q}\rangle, \quad \text{(C2)}$$

and the partial wave expansion,

$$\langle \vec{q}|A|\vec{q}'\rangle = A(q, q', \hat{q}.\hat{q}') = \frac{1}{4\pi} \sum_l (2l+1) A_l(q, q') P_l(\hat{q}.\hat{q}'), \quad \text{(C3)}$$

where $P_l(x)$ is the Legendre polynomial of order l, (C1) reads

$$\Omega_s = \frac{1}{64\pi^5\beta^2} \sum_{J^P} (2J+1) \sum_{\mathcal{C}} \dim \mathcal{C} \Bigg(\beta \int_{2m_g}^{\infty} d\epsilon \epsilon^3 \sqrt{\frac{\epsilon^2}{4} - m_g^2} K_1(\beta\epsilon) \,\mathrm{Re}\mathcal{T}_{J^P}(\epsilon; q_\epsilon, q_\epsilon) - \frac{1}{16\pi^2} \int_{2m_g}^{\infty} d\epsilon \epsilon^4 \left(\frac{\epsilon^2}{4} - m_g^2\right) K_2(\beta\epsilon) [\mathrm{Re}\mathcal{T}_{J^P}(\epsilon; q_\epsilon, q_\epsilon)(\mathrm{Im}\mathcal{T}_{J^P}(\epsilon; q_\epsilon, q_\epsilon))'] + \frac{1}{16\pi^2} \int_{2m_g}^{\infty} d\epsilon \epsilon^4 \left(\frac{\epsilon^2}{4} - m_g^2\right) K_2(\beta\epsilon) [(\mathrm{Re}\mathcal{T}_{J^P}(\epsilon; q_\epsilon, q_\epsilon))' \,\mathrm{Im}\mathcal{T}_{J^P}(\epsilon; q_\epsilon, q_\epsilon)] \Bigg). \quad \text{(C4)}$$

[1] J. C. Collins and M. J. Perry, Phys. Rev. Lett. **34**, 1353 (1975).
[2] E. V. Shuryak, Phys. Rep. **61**, 71 (1980).
[3] D. Cabrera and R. Rapp, Phys. Rev. D **76**, 114506 (2007).
[4] R. Dashen, S.-K. Ma, and H. J. Bernstein, Phys. Rev. **187**, 345 (1969); Phys. Rev. A **6**, 851(E) (1972).
[5] M. I. Gorenstein and S. N. Yang, Phys. Rev. D **52**, 5206 (1995).
[6] F. Buisseret and G. Lacroix, Eur. Phys. J. C **70**, 1051 (2010).
[7] J.-P. Blaizot, Nucl. Phys. **A751**, 139 (2005).
[8] M. Bluhm, B. Kämpfer, and K. Redlich, Phys. Rev. C **84**, 025201 (2011); Phys. Lett. B **709**, 77 (2012).
[9] K. Fukushima and C. Sasaki, arXiv:1301.6377.
[10] L. Tolós, D. Cabrera, and A. Ramos, Phys. Rev. C **78**, 045205 (2008).
[11] M. Mannarelli and R. Rapp, Phys. Rev. C **72**, 064905 (2005).
[12] H. van Hees, M. Mannarelli, V. Greco, and R. Rapp, Phys. Rev. Lett. **100**, 192301 (2008).
[13] K. Huggins and R. Rapp, Nucl. Phys. **A896**, 24 (2012).
[14] M. Pepe and U.-J. Wiese, Nucl. Phys. **B768**, 21 (2007).
[15] V. Goloviznin and H. Satz, Z. Phys. C **57**, 671 (1993).
[16] F. Brau and F. Buisseret, Phys. Rev. D **79**, 114007 (2009).
[17] S. Gupta, K. Hübner, and O. Kaczmarek, Phys. Rev. D **77**, 034503 (2008).
[18] J. Fuchs and C. Schweigert, *Symmetries, Lie Algebras and Representations* (Cambridge University Press, Cambridge, England, 1997).
[19] N. Boulanger, F. Buisseret, V. Mathieu, and C. Semay, Eur. Phys. J. A **38**, 317 (2008).
[20] M. Jacob and G. C. Wick, Ann. Phys. (N.Y.) **7**, 404 (1959).
[21] D. R. Giebink, Phys. Rev. C **32**, 502 (1985).
[22] V. Mathieu, F. Buisseret, and C. Semay, Phys. Rev. D **77**, 114022 (2008); F. Buisseret, V. Mathieu, and C. Semay, Phys. Rev. D **80**, 074021 (2009).
[23] T. Barnes, Z. Phys. C **10**, 275 (1981).
[24] V. Mathieu, N. Kochelev, and V. Vento, Int. J. Mod. Phys. E **18**, 1 (2009), and references therein.
[25] M. I. Haftel and F. Tabakin, Nucl. Phys. **A158**, 1 (1970).
[26] F. Buisseret and G. Lacroix, Phys. Lett. B **705**, 405 (2011).
[27] B. Lucini, M. Teper, and U. Wenger, J. High Energy Phys. 02 (2005) 033.
[28] L. Lipták and Š. Olejník, Phys. Rev. D **78**, 074501 (2008); B. H. Wellegehausen, A. Wipf, and C. Wozar, Phys. Rev. D **83**, 016001 (2011).
[29] F. Buisseret, Eur. Phys. J. C **71**, 1651 (2011).
[30] G. 't Hooft, Nucl. Phys. **B72**, 461 (1974).
[31] A. Armoni, M. Shifman, and G. Veneziano, Nucl. Phys. **B667**, 170 (2003); Phys. Rev. Lett. **91**, 191601 (2003).
[32] O. Kaczmarek, F. Karsch, P. Petreczky, and F. Zantow, Phys. Lett. B **543**, 41 (2002).
[33] M. Asakawa and T. Hatsuda, Phys. Rev. Lett. **92**, 012001 (2004).
[34] W. M. Alberico, A. Beraudo, A. De Pace, and A. Molinari, Phys. Rev. D **72**, 114011 (2005).
[35] C.-Y. Wong and H. W. Crater, Phys. Rev. D **75**, 034505 (2007).
[36] F. Riek and R. Rapp, Phys. Rev. C **82**, 035201 (2010).
[37] A. Mocsy and P. Petreczky, Phys. Rev. D **73**, 074007 (2006).

[38] J.-P. Blaizot, E. Iancu, and A. Rebhan, Phys. Lett. B **470**, 181 (1999); Phys. Rev. D **63**, 065003 (2001).
[39] A. Peshier, B. Kämpfer, O. P. Pavlenko, and G. Soff, Phys. Rev. D **54**, 2399 (1996).
[40] M. Ruggieri, P. Alba, P. Castorina, S. Plumari, C. Ratti, and V. Greco, Phys. Rev. D **86**, 054007 (2012).
[41] A. Cucchieri and T. Mendes, Phys. Rev. D **81**, 016005 (2010).
[42] O. Oliveira and P. Bicudo, J. Phys. G **38**, 045003 (2011).
[43] J. M. Cornwall, Phys. Rev. D **26**, 1453 (1982).
[44] D. Binosi and J. Papavassiliou, Phys. Rep. **479**, 1 (2009).
[45] A. C. Aguilar, D. Binosi, J. Papavassiliou, and J. Rodriguez-Quintero, Phys. Rev. D **80**, 085018 (2009); A. C. Aguilar, D. Binosi, and J. Papavassiliou, J. High Energy Phys. 07 (2010) 002.
[46] H. Reinhardt, D. R. Campagnari, and A. P. Szczepaniak, Phys. Rev. D **84**, 045006 (2011).
[47] E. Megias, E. R. Arriola, and L. L. Salcedo, Phys. Rev. D **75**, 105019 (2007); **80**, 056005 (2009).
[48] C. J. Morningstar and M. J. Peardon, Phys. Rev. D **60**, 034509 (1999); Y. Chen *et al.*, Phys. Rev. D **73**, 014516 (2006).
[49] G. S. Bali, Phys. Rep. **343**, 1 (2001); C. Semay, Eur. Phys. J. A **22**, 353 (2004); M. Cardoso and P. Bicudo, Phys. Rev. D **78**, 074508 (2008).
[50] P. de Forcrand and O. Philipsen, Phys. Lett. B **475**, 280 (2000).
[51] G. S. Bali and A. Pineda, Phys. Rev. D **69**, 094001 (2004).
[52] A. Szczepaniak, E. S. Swanson, C.-R. Ji, and S. R. Cotanch, Phys. Rev. Lett. **76**, 2011 (1996); A. P. Szczepaniak and E. S. Swanson, Phys. Lett. B **577**, 61 (2003).
[53] W. E. Caswell, Phys. Rev. Lett. **33**, 244 (1974).
[54] B. Lucini, A. Rago, and E. Rinaldi, J. High Energy Phys. 08 (2010) 119.
[55] H. B. Meyer, Phys. Rev. D **80**, 051502(R) (2009).
[56] M. Caselle, L. Castagnini, A. Feo, F. Gliozzi, and M. Panero, J. High Energy Phys. 06 (2011) 142.
[57] B. Lucini, M. Teper, and U. Wenger, J. High Energy Phys. 01 (2004) 061.
[58] J. Braun, A. Eichhorn, H. Gies, and J. M. Pawlowski, Eur. Phys. J. C **70**, 689 (2010).
[59] A. Maas, J. High Energy Phys. 02 (2011) 076.
[60] N. Ishii, H. Suganuma, and H. Matsufuru, Phys. Rev. D **66**, 094506 (2002).
[61] X.-F. Meng, G. Li, Y.-J. Zhang, Y. Chen, C. Liu, Y.-B. Liu, J.-P. Ma, and J.-B. Zhang, Phys. Rev. D **80**, 114502 (2009).
[62] M. Panero, Phys. Rev. Lett. **103**, 232001 (2009).
[63] S. Borsányi, G. Endrődi, Z. Fodor, S. D. Katz, and K. K. Szabó, J. High Energy Phys. 07 (2012) 056.
[64] A. Dumitru, Y. Guo, Y. Hidaka, C. P. K. Altes, and R. D. Pisarski, Phys. Rev. D **86**, 105017 (2012).
[65] T. Yépez-Martínez, A. P. Szczepaniak, and H. Reinhardt, Phys. Rev. D **86**, 076010 (2012).
[66] B. Lucini and M. Teper, Phys. Rev. D **64**, 105019 (2001).
[67] H. Satz, arXiv:hep-ph/0602245; V. V. Dixit, Mod. Phys. Lett. A **05**, 227 (1990).
[68] J. Engels, J. Fingberg, K. Redlich, H. Satz, and M. Weber, Z. Phys. C **42**, 341 (1989).